

Cementitious Rad-Waste Monoliths, DUO_2 Aggregates in Shielding, and Yucca Tunnel Liners

Les Dole and Catherine Mattus

**TC RWD – Use of Concrete in Radioactive
Waste Disposal Facilities**

**RILEM - Réunion Internationale des Laboratoires
et Experts des Matériaux, Systèmes de
Constructions et Ouvrages**

Northwestern University, Evanston, Illinois

October 5–6, 2004

Contact: dolelr@ornl.gov

865-576-4319

**OAK RIDGE NATIONAL LABORATORY
U. S. DEPARTMENT OF ENERGY**

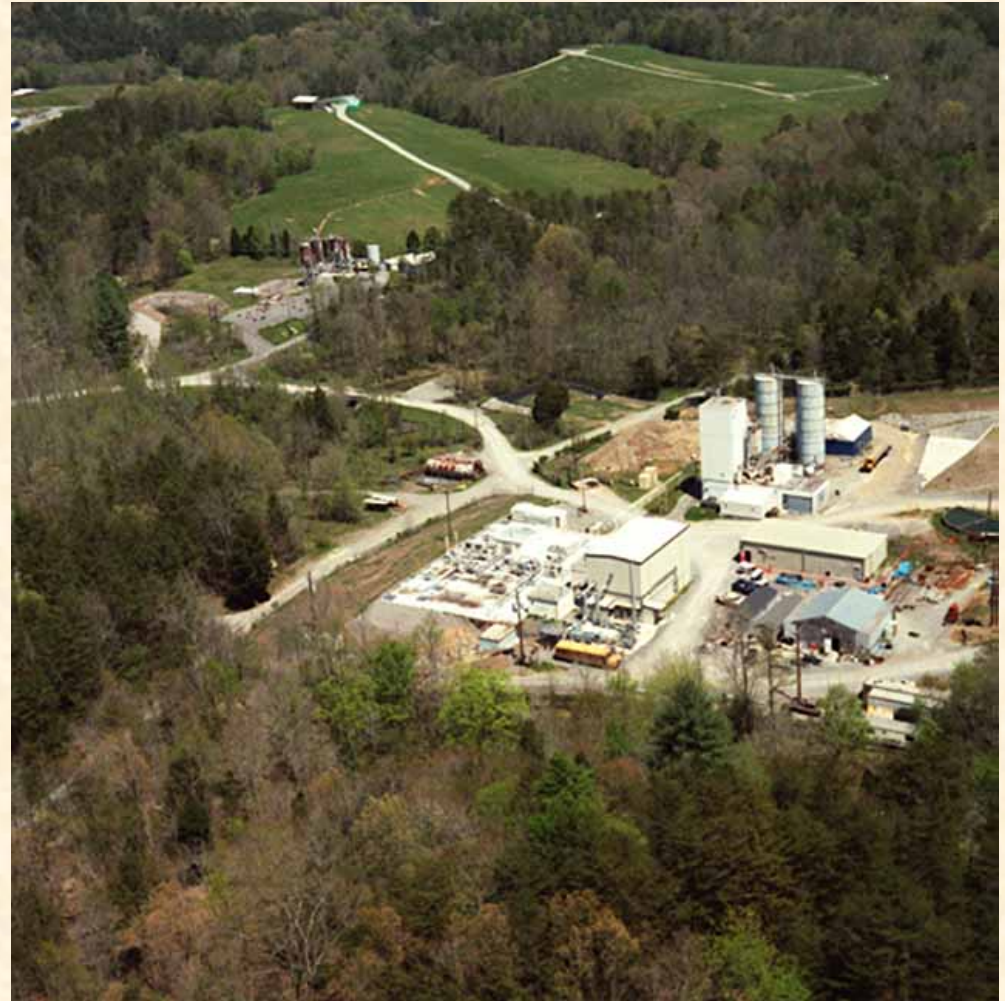
ORNL Experience with Cementitious Waste Forms

- **>40 years of treatability, formulation, and process studies of disposal of rad and chemical waste from across the DOE complex**
- **Processes to treat >50 million curies of rad waste and >0.5 million tons of contaminated soils**
- **Experience in overcoming interactions of waste components with reaction paths of cementitious materials**
- **Experience in characterizing performance and durability of products**

L. R. Dole and T. H. Row, [Development Programs in the United States of America for the Application of Cement-Based Grouts in Radioactive Waste Management](#), CEA1982 presented by T. H. Row at the Second Meeting of the Bilateral Agreement on Radioactive Waste Management between the United States Department of Energy and the French Commissariat A L'Energy Atomique, Paris, France, June 1984

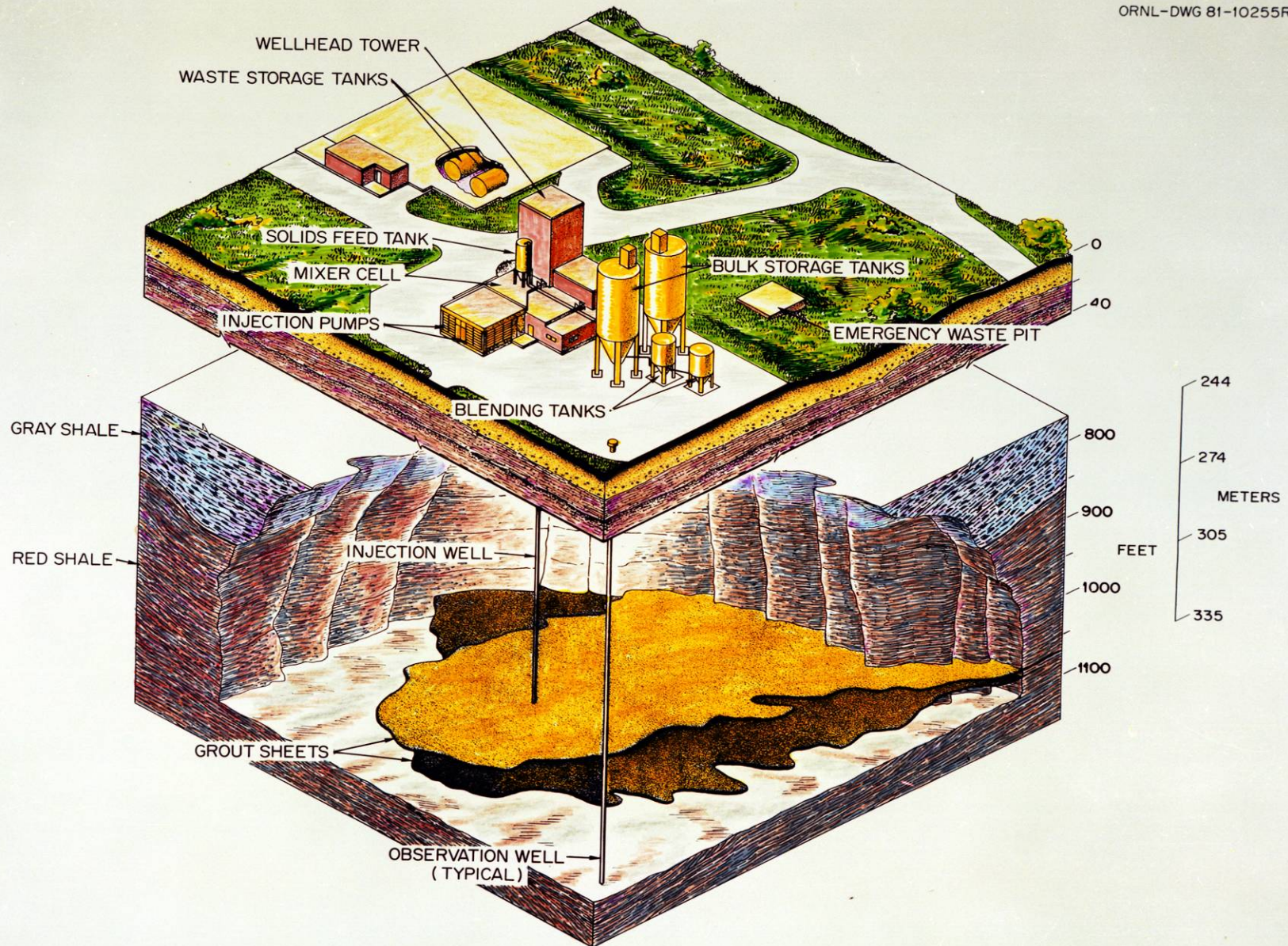
ORNL Hydrofracture Plants

- Inject fluid grouts into shale formation at about 1,000 ft using oil field technology
- Disposed of annual liquid waste in 10 hr
- Disposal costs for about \$1.25/gal



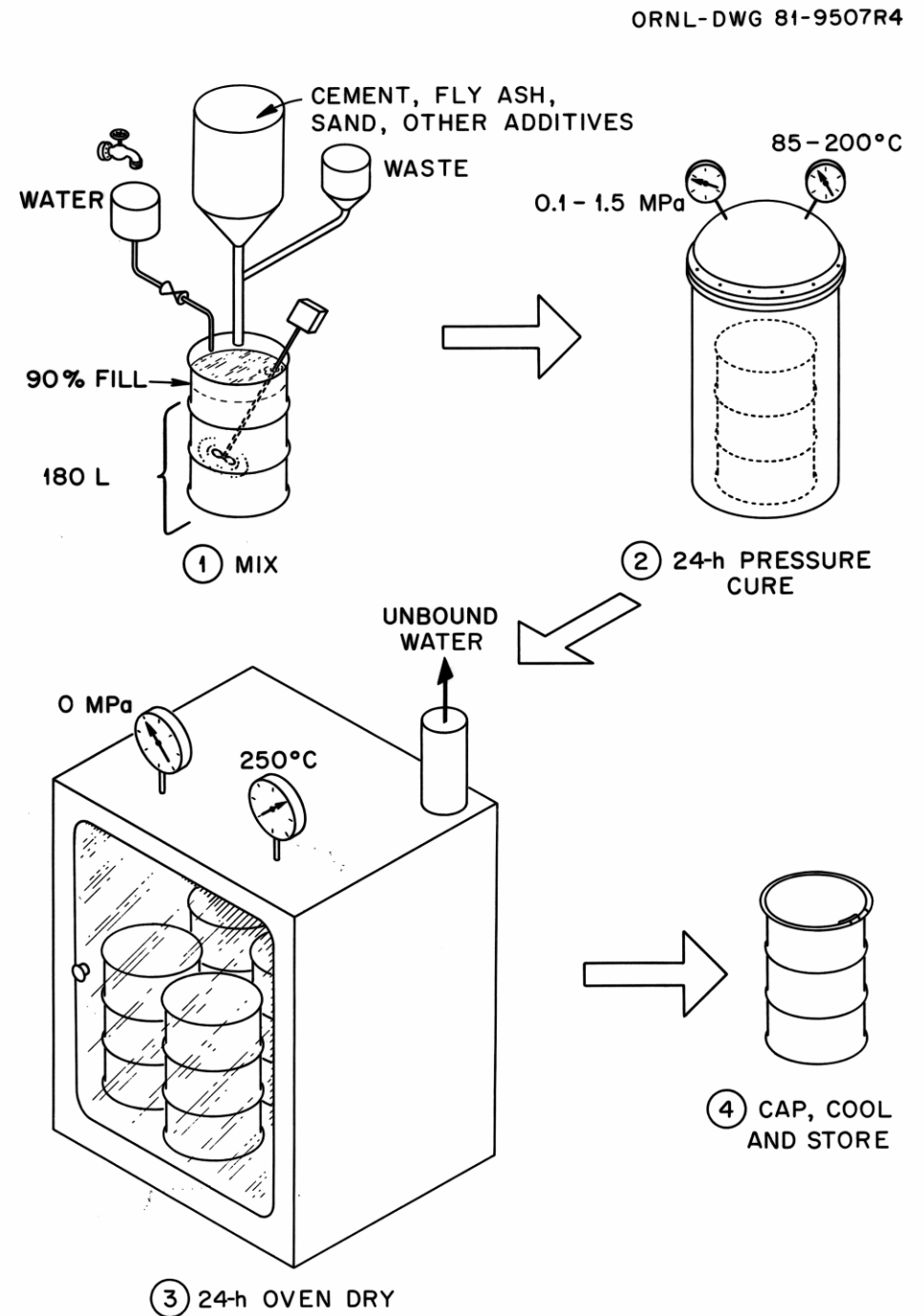
Cross Section of Hydrofracture

ORNL-DWG 81-10255RC



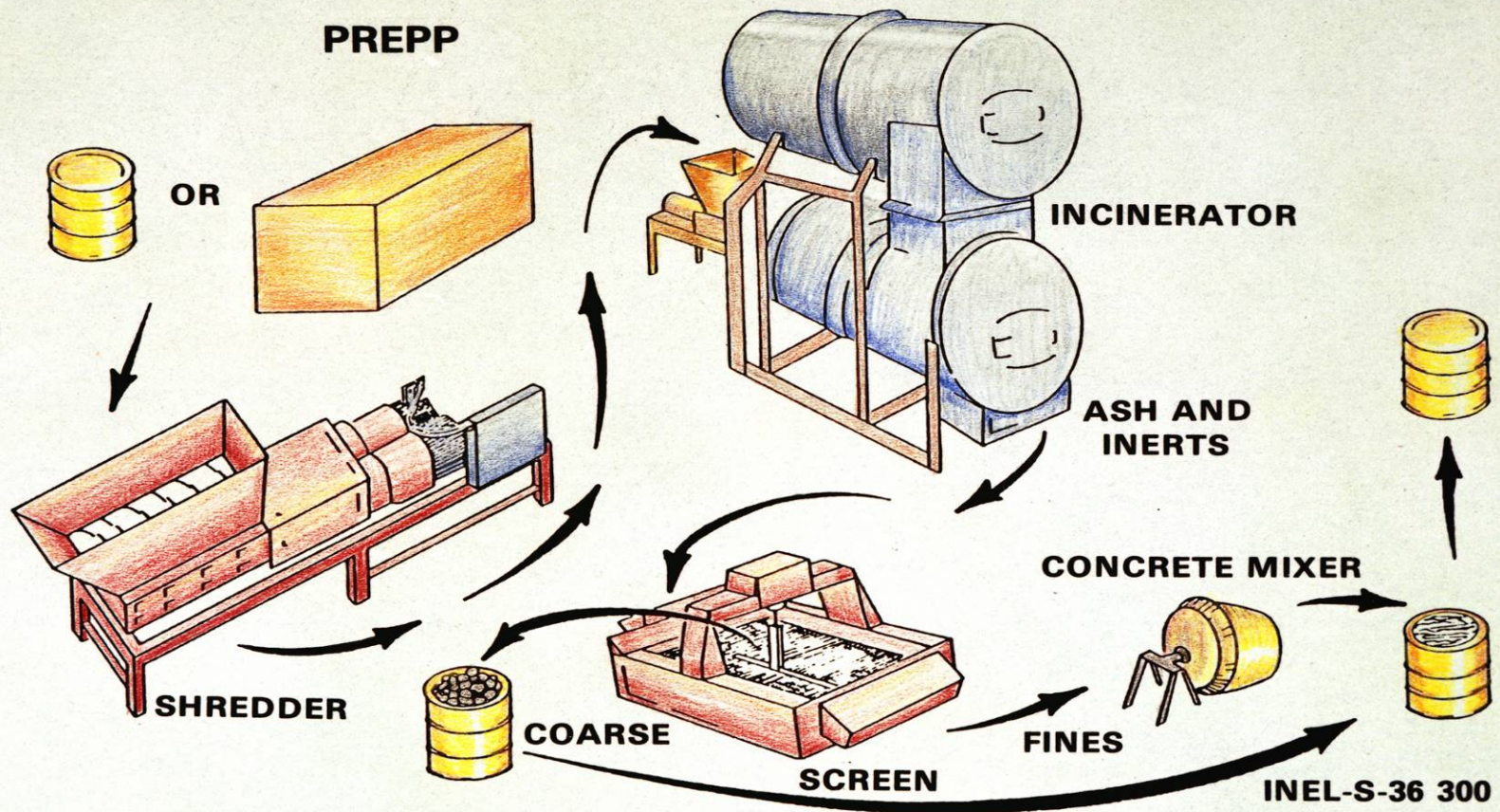
FUETAP - High-level Waste Cementitious Monoliths Formed Under Elevated Temperature and Pressure

OAK RIDGE NATIONAL LABORATORY
U. S. DEPARTMENT OF ENERGY



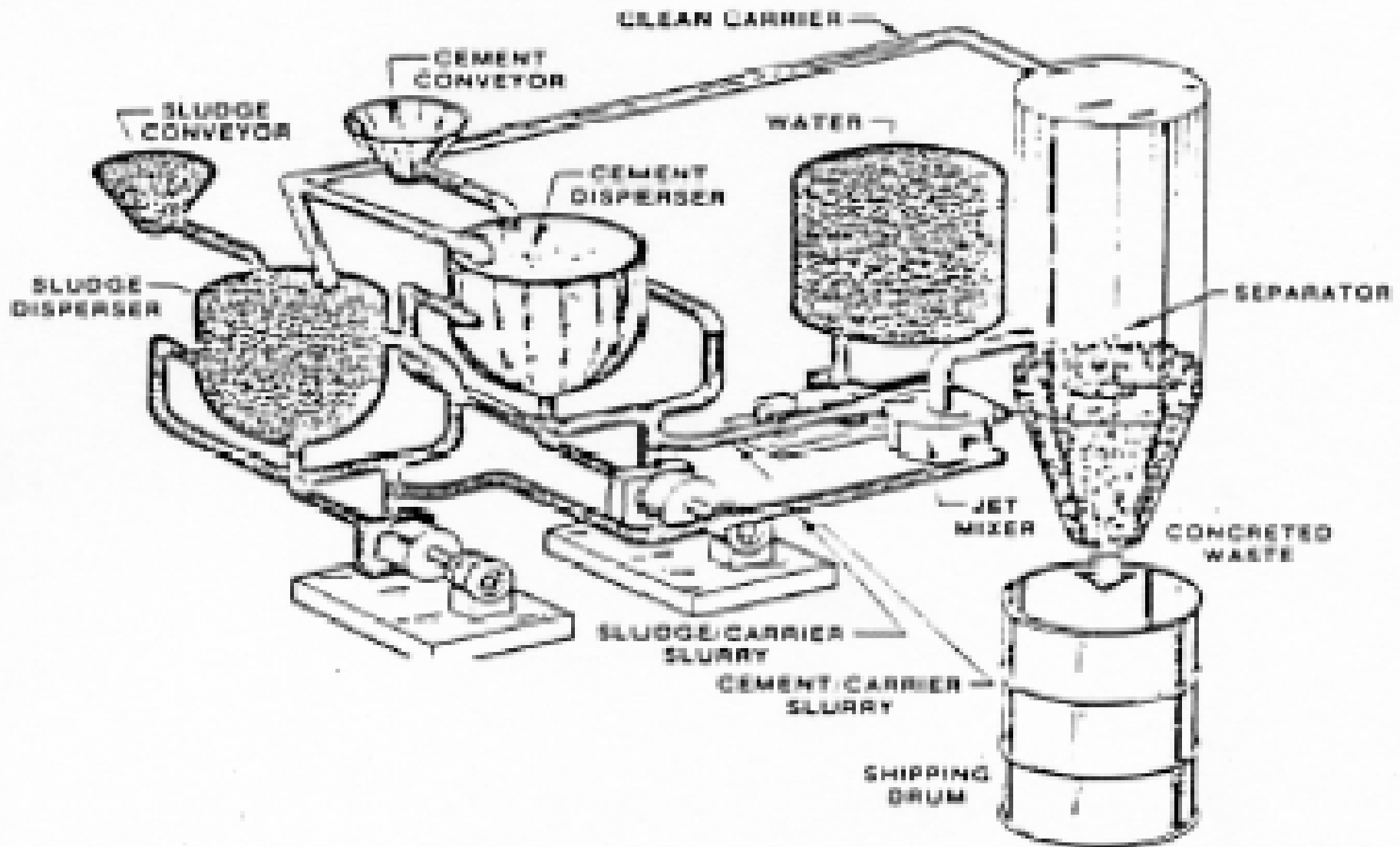
Ash Trash Solidification and Encapsulation

ORNL-DWG 82-19628



**PROCESS EXPERIMENTAL PILOT PLANT
(PREPP) FLOW DIAGRAM**

Non-Aqueous Mixing Waste and Binders



Leach Tests with Analysis to Compare and Formulate Better Waste Forms

- **Complex alumina-silicates with fine textured mineral phases and large fraction of amorphous hydrosilicate phase, both of which slowly undergoes diagenesis and contact metamorphism over centuries and millennia**
- **Leaches matrix components at different rates and results in a complex series of solution reactions with groundwater adjacent to the surface that redeposit minerals**

Short-Term Leach Testing to Assess Impacts of Waste Constituents and Formula Constituents

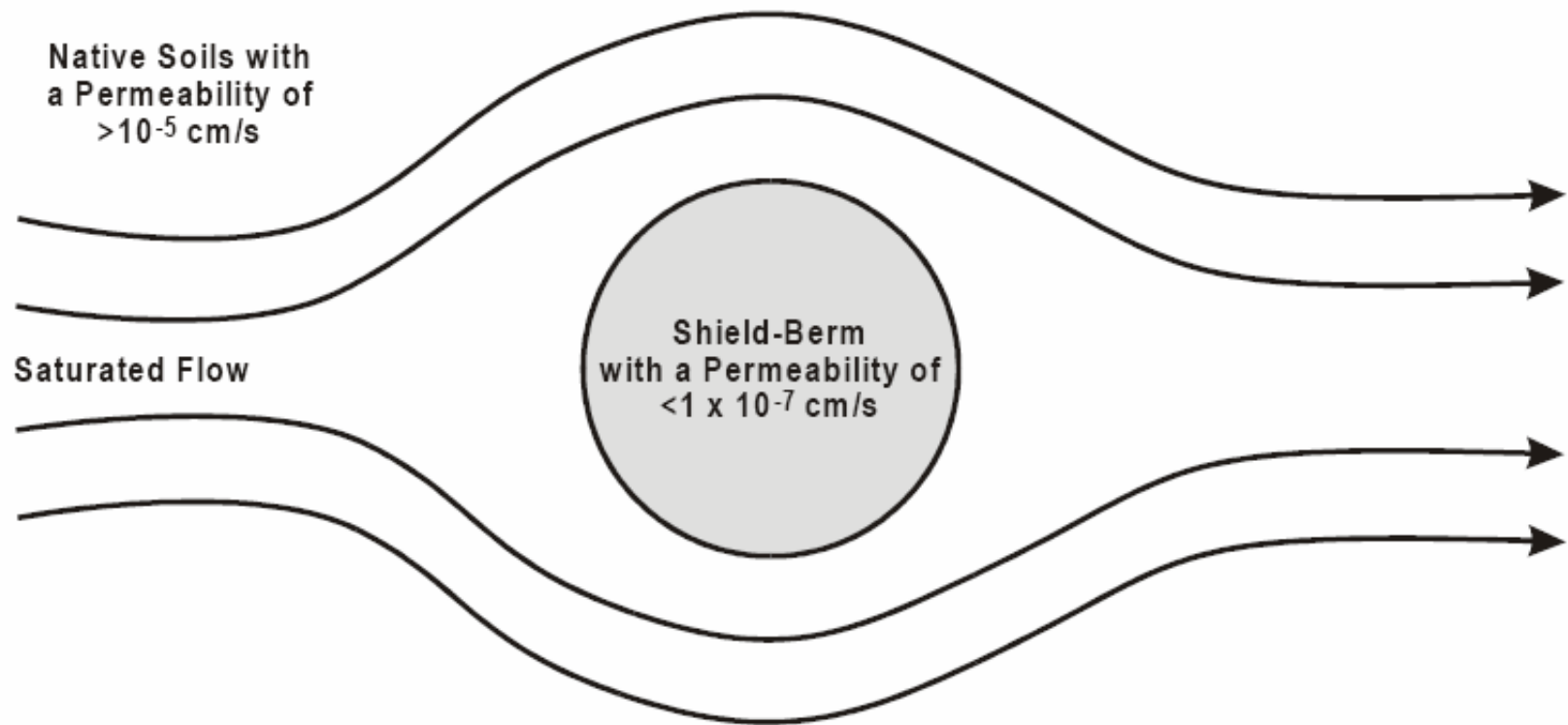
- **Choices of cement types**
- **Choices of admixtures to change:**
 - **Ca/Si ratios**
 - **Al/Si ratios**
 - **Permeability (H₂O, O₂, SO₄⁼, Cl⁻, etc)**
 - **Internal ion exchange capacity**
 - **Reducing conditions (Eh/Ph regime)**

Test Performances at Hydraulic Extremes

- **Quasi-static flow (episodic saturation)**
 - Solubility control
 - Ion exchange equilibrium
 - Source-term = $C_{\text{sat}} \times \text{Flow}$
- **Dynamic (monolith permeability $< 1/100$ soil)**
 - Advection of saturated groundwater
 - Release to groundwater limited by diffusion within the monolith
 - Source-term = $A_0 \{S/V\} (D_{\text{diffusion}}/\text{time})^{1/2}$

A Relatively Impermeable Monolith has No Advection

A Differential Permeability of 100 Times Ensures that Saturated Flow By-Passes the Matrix



A Practical Model for the "Effective" Diffusion Coefficient

$$K_{MB} = \frac{\left[\frac{\text{mole of species}}{\text{mass of porous solid}} \right]}{\left[\frac{\text{mole of species}}{\text{volume of liquid}} \right]}$$

$$D_e = \frac{D_f}{\tau^2 \cdot \left[1 + \rho_b \cdot \left[\frac{(1-\epsilon)}{\epsilon} \right] \cdot K_{MB} \right]}$$

where

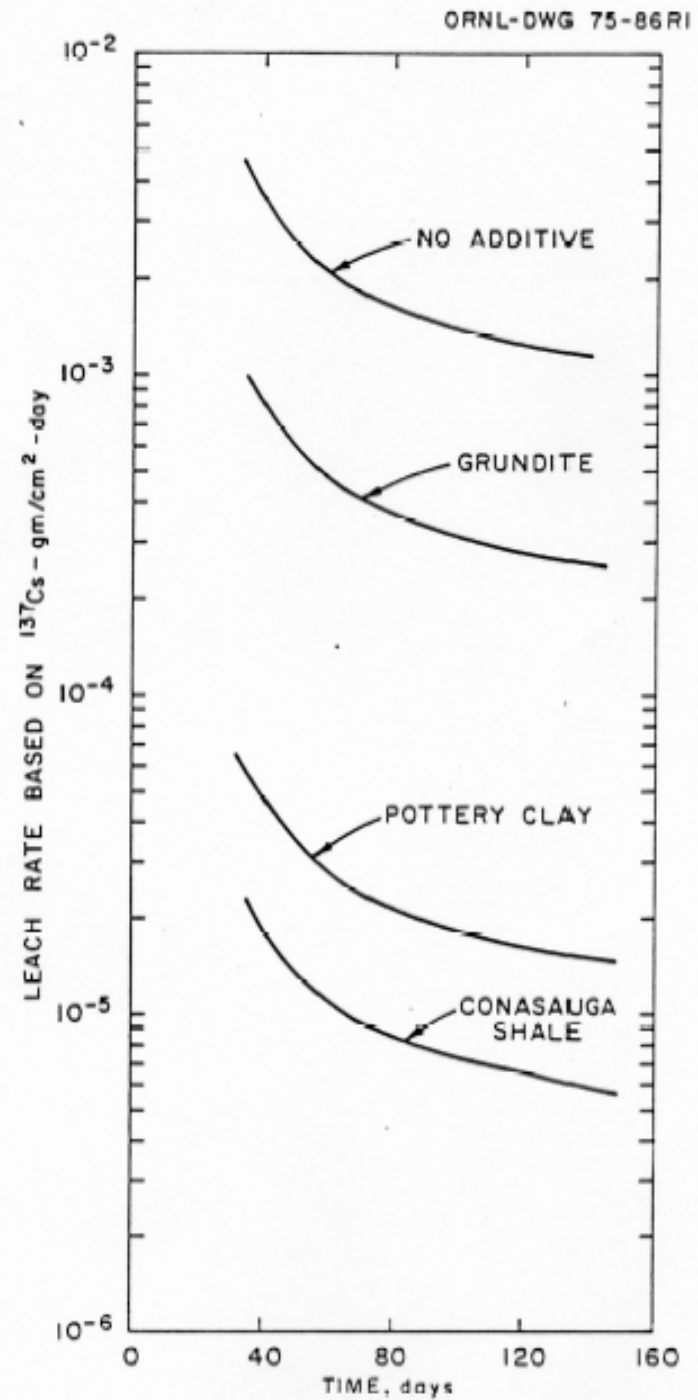
τ = tortuosity, *dimensionless* (This study assumed that τ was equal to 1.47 for the compacted berm soils.)

ρ_b = bulk density of porous soil, g/cm³

ϵ = average *effective* open porosity, *dimensionless*.

Effects of Additives on the Leaching of ^{137}Cs from Hydrofracture Grouts

OAK RIDGE NATIONAL LABORATORY
U. S. DEPARTMENT OF ENERGY



500 Year Release Model for Sr-90 Activity from Grouted GAAT Sludge from Gunitite Tank W9

Effective diffusion Coefficient:

$$D_e := \left(2.6 \cdot 10^{-13}\right) \cdot \frac{\text{cm}^2}{\text{sec}} \quad \begin{array}{l} * \text{Data from similar hydrofracture grouts} \\ * \text{assumes most activity is Sr-90} \end{array}$$

Time iteration

$$i := 0, 10.. 500$$

$$t_i := i \cdot \text{yr}$$

Surface to Volume:

$$\frac{S}{V} = 5.125 \text{cm}^{-1} \quad \begin{array}{l} * \text{Assumes entire surface on the monolith is exposed to flowing ground water.} \\ * \text{No credit is given for the existing tank walls.} \end{array}$$

Infinite slab diffusion model: $FI(t) := 2 \cdot \frac{S}{V} \cdot \sqrt{\frac{D_e \cdot t}{\pi}}$ * calculates a conservative overestimate of release

$$t_2 := \left(0.2 \cdot \frac{V}{S \cdot 2}\right)^2 \cdot \left(\frac{\pi}{D_e}\right) \quad t_2 = 145.805 \text{yr} \quad FI(t_2) = 0.2 \quad \begin{array}{l} * \text{On-set of geometry} \\ * \text{specific effects} \end{array}$$

$$t_5 := \left(0.5 \cdot \frac{V}{S \cdot 2}\right)^2 \cdot \left(\frac{\pi}{D_e}\right) \quad t_5 = 911.278 \text{yr} \quad FI(t_5) = 0.5 \quad \begin{array}{l} * \text{Chemical half-life in} \\ * \text{monolith} \end{array}$$

Onset of Geometric Model at FC=0.2

Nestor, C. W., Jr., *Diffusion from Solid Cylinders*, **ORNL/SDTM-84**, Lockheed Martin Energy Research Corp., Oak Ridge National Laboratory, Oak Ridge, Tennessee, January 1980.

$$\alpha_j := \frac{\text{root}(J_0(j), j)}{a}$$

D_e = effective diffusion coefficient, cm² s⁻¹

a = cylinder radius, cm

j = j th positive root of a zero-order Bessel function [$J_0(m)$]

L = cylinder half-height, cm.

Diffusion from a Cylinder:

$$FC(t) := 1 - \frac{32}{\pi^2 \cdot a^2} \cdot \sum_n \sum_j \frac{e^{-\left[D_e \cdot \left[(\alpha_j)^2 + (2 \cdot n - 1)^2 \cdot \frac{\pi^2}{4 \cdot L^2} \right] \cdot t \right]}}{(2 \cdot n - 1)^2 \cdot (\alpha_j)^2}$$

$$FC(t_2) = 0.223 \quad FS(t) := \text{if}(t > t_2, FC(t), FI(t))$$

$$F_i := FS(t_i)$$

$$FI_1 := FI(t_i)$$

Example: Diffusion Controlled Release of ⁹⁰Sr from a Monolith

Fraction Released

$$F_{30} = 0.091$$

$$F_{300} = 0.303$$

$$F_{500} = 0.379$$

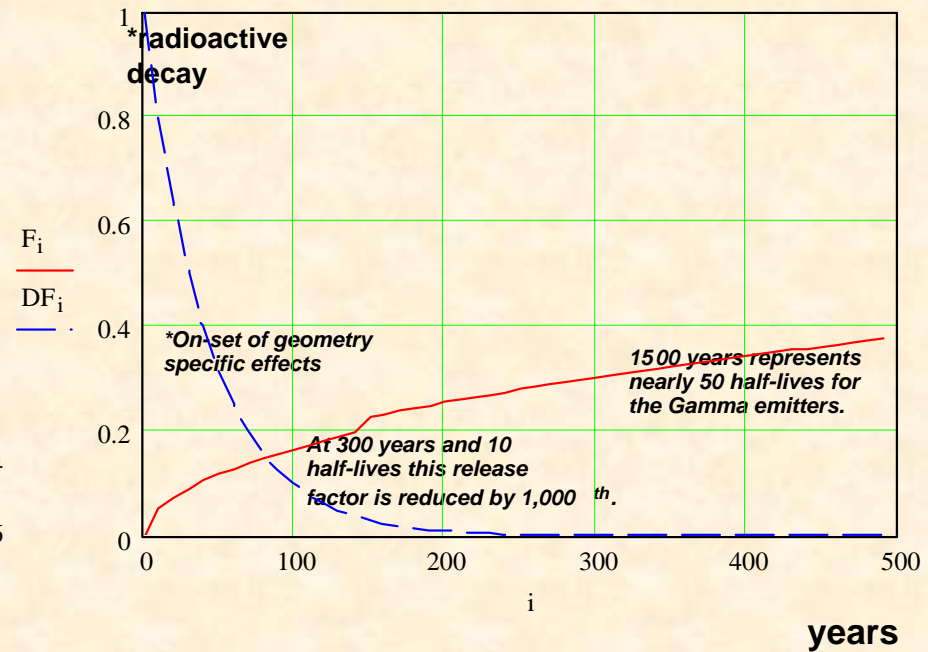
Radioactive Decay Factor

$$DF_{30} = 0.5$$

$$DF_{300} = 9.766 \times 10^{-4}$$

$$DF_{500} = 9.612 \times 10^{-6}$$

CURIE RELEASE FROM W9 MONOLITH as Sr-90



Combination of Decay and Diffusion Controlled Release

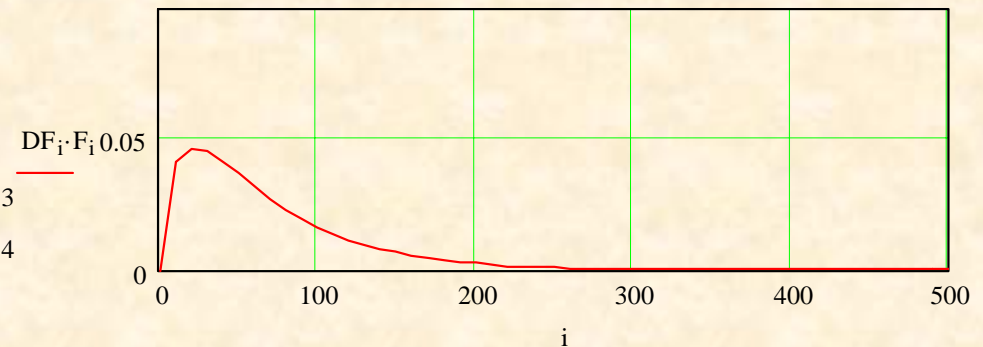
Decay Fraction X Release Fraction

$$DF_{30} \cdot F_{30} = 0.045$$

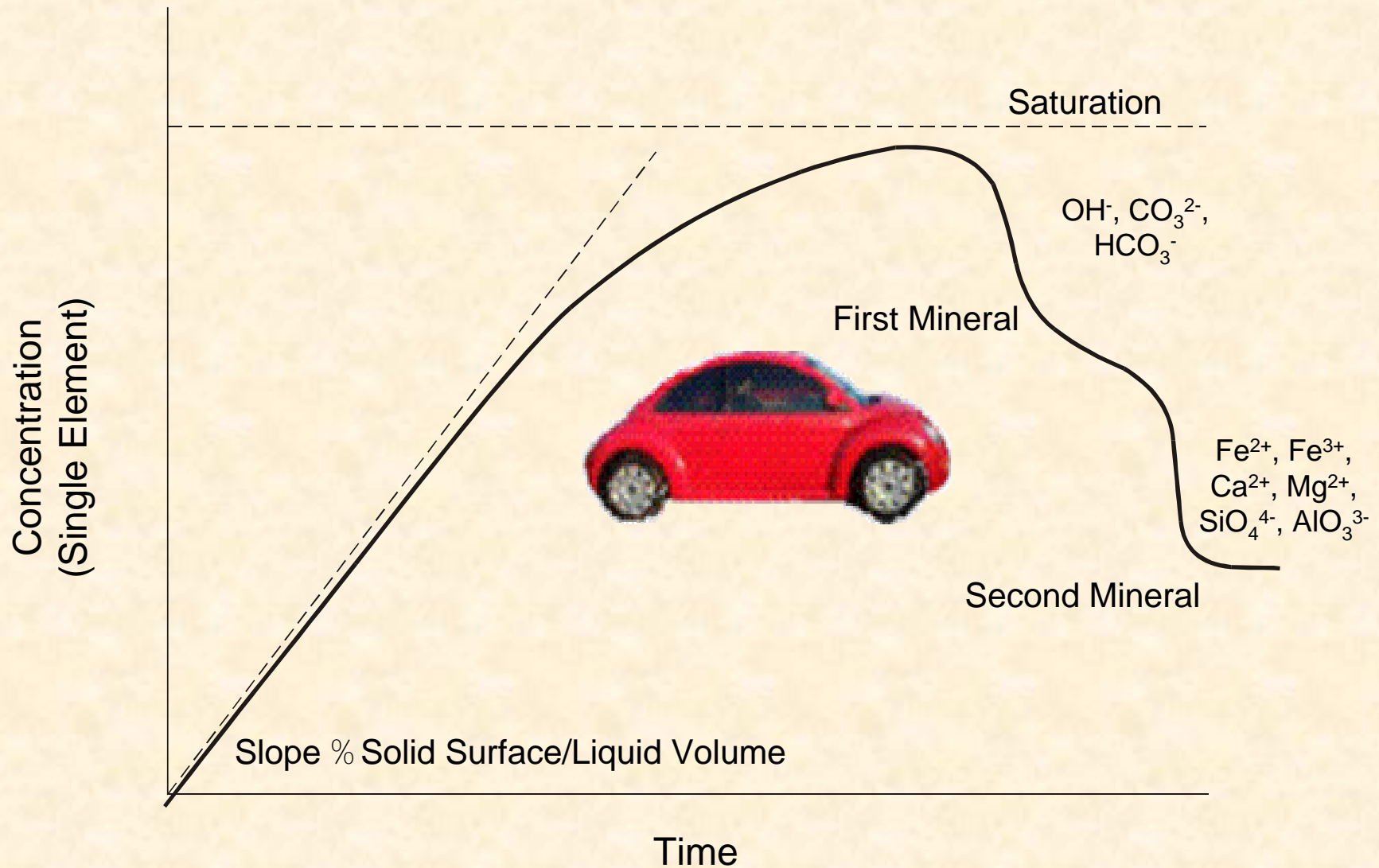
$$DF_{90} \cdot F_{90} = 0.02$$

$$DF_{150} \cdot F_{150} = 7.047 \times 10^{-3}$$

$$DF_{300} \cdot F_{300} = 2.955 \times 10^{-4}$$

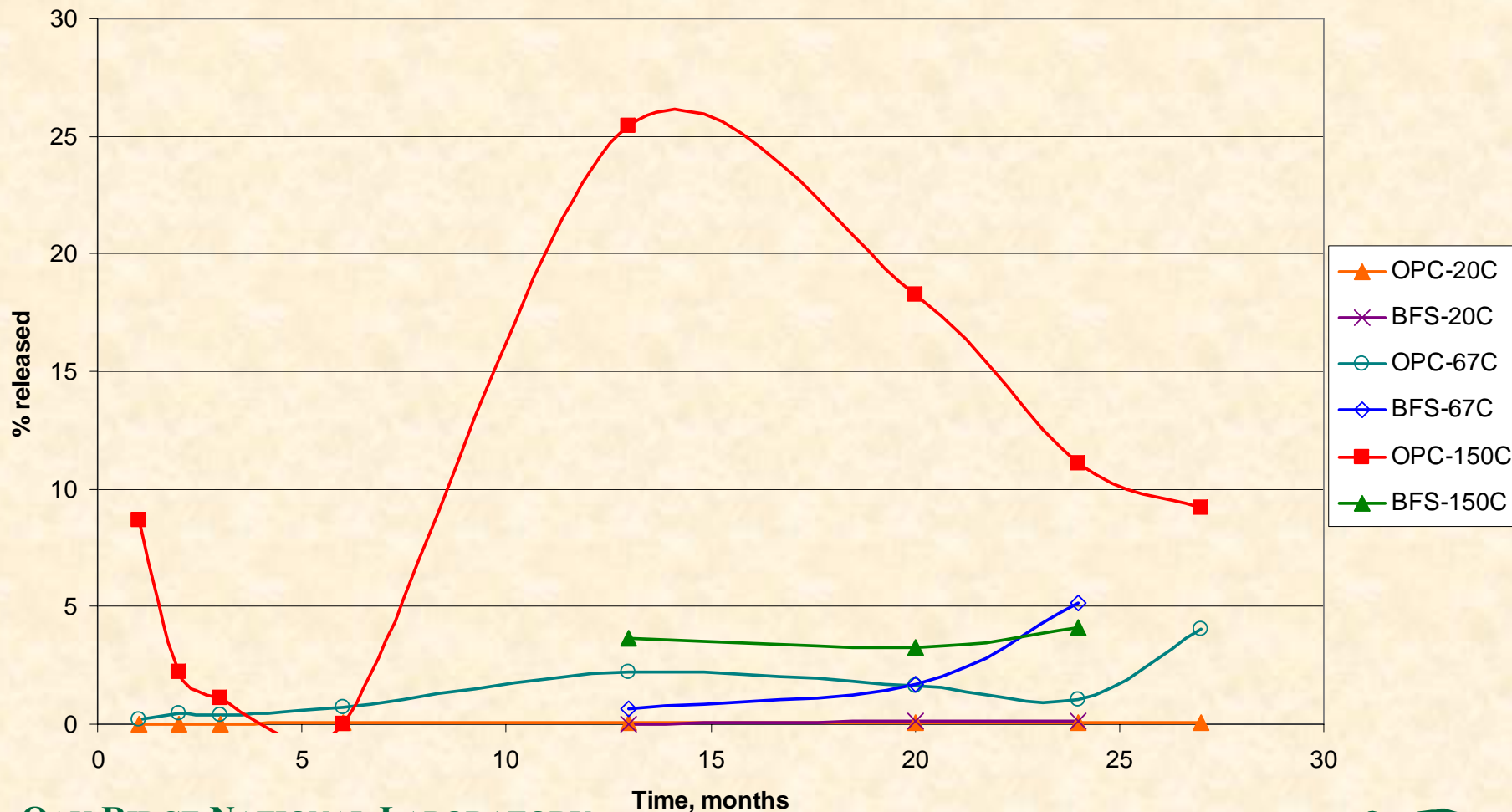


Static Leaching with Secondary Mineral Formation



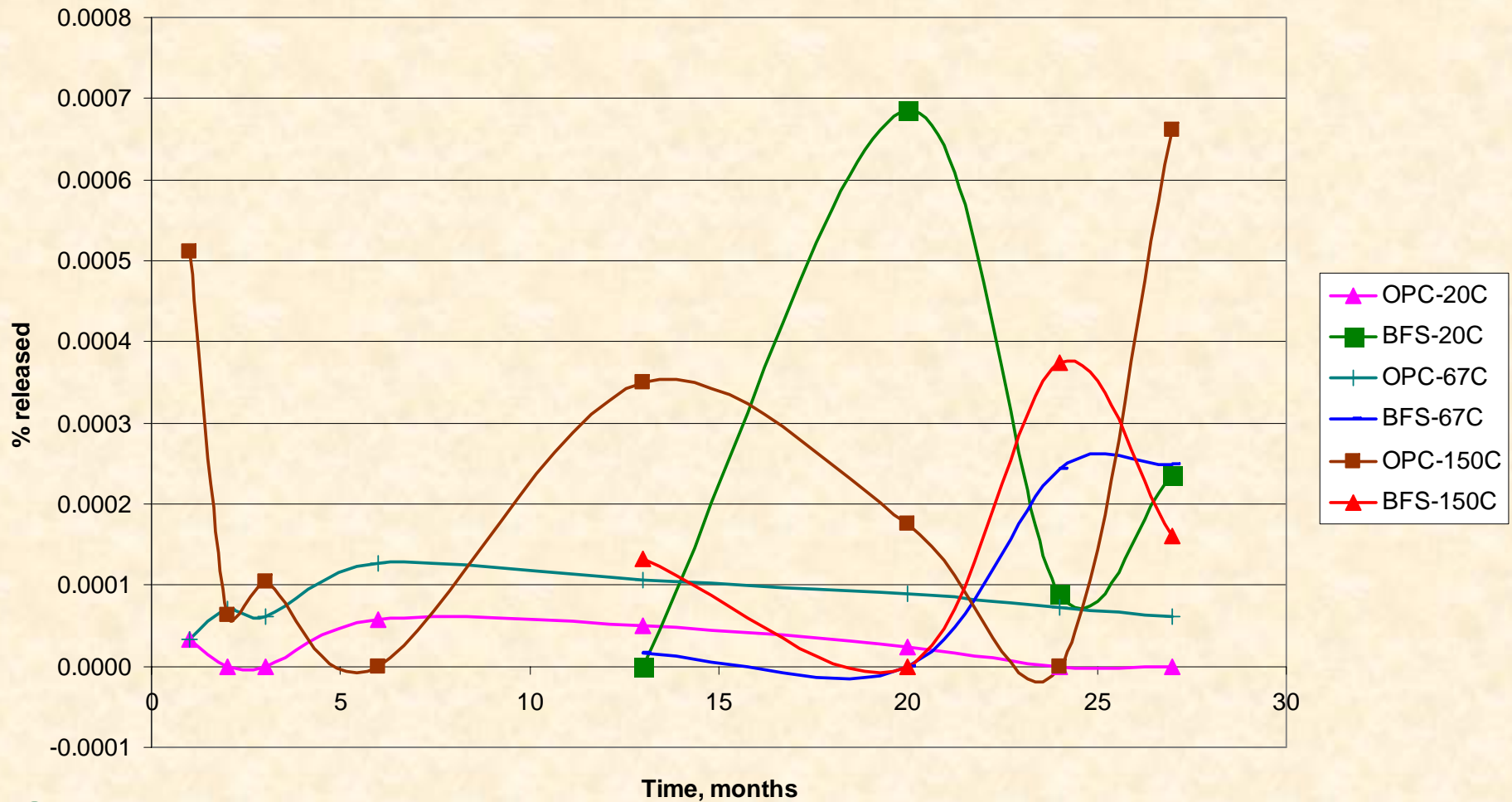
Si Released from DUAGG into Cement and Blast-Furnace Slag Porewater

Silicon released (%) from DUAGG pellet



U Released from DUAGG into Cement and Blast-Furnace Slag Porewater

Uranium released (%) from DUAGG pellet



Conclusions?

Short-term leach testing is conservative IF:

- Test does not allow for the effects of secondary minerals, which are**
 - Highly selective for contaminant species**
 - Forms protective diffusion surface-barriers**

- The monolith matrix is relatively stable in the geochemistry of the disposal horizon**
 - Shares same regions of the geochemical stability fields**
 - Has similar $\text{SiO}_2\text{-Al}_2\text{O}_3$ composition ranges**

- Ultimate mechanisms of leaching, alterations, and weathering are controlled by solid-diffusion rates**

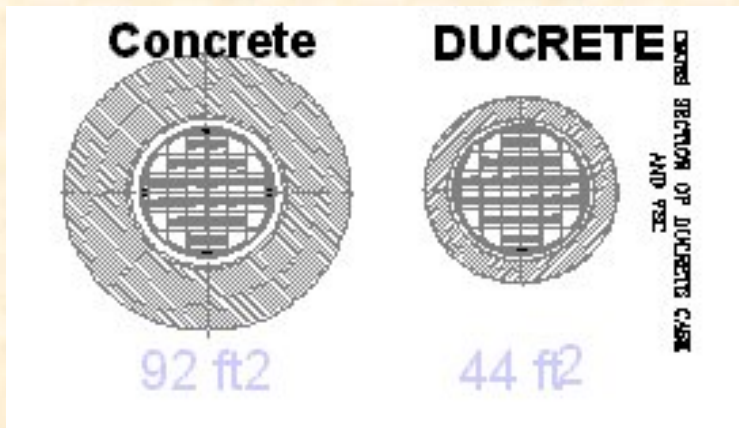
DUAGG Briquettes are Stabilized DU Aggregates with Basalt Sintering Agent



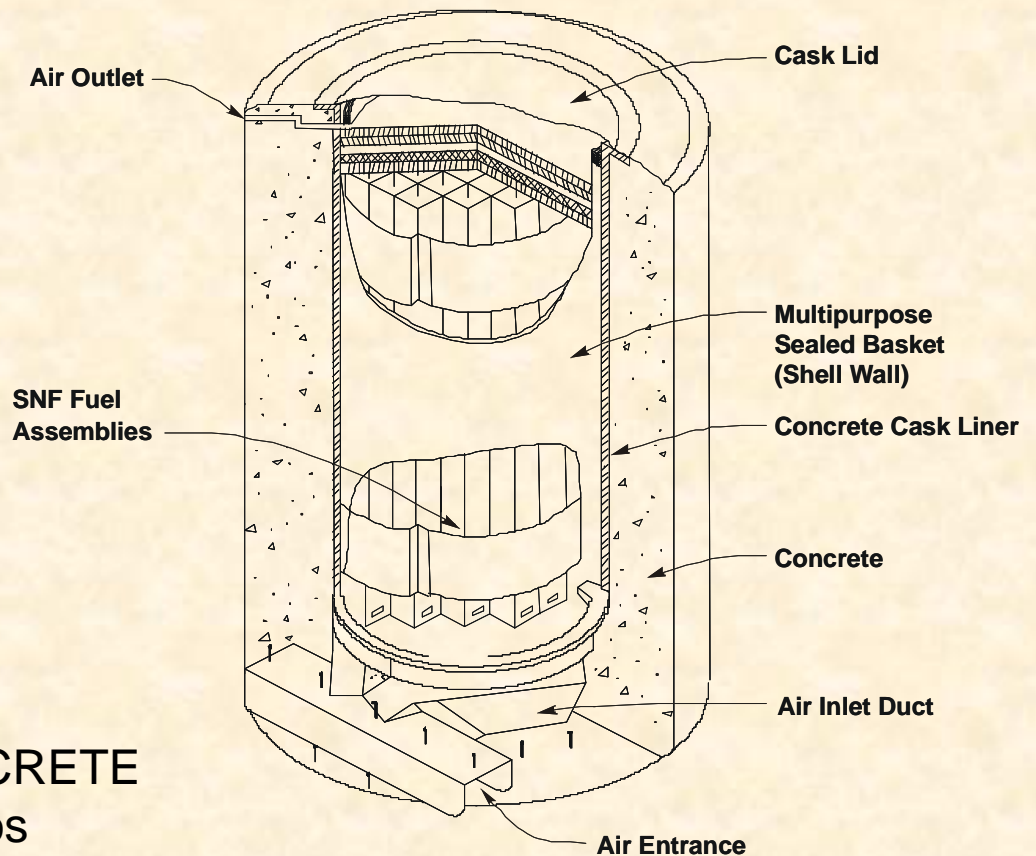
Briquettes are pressed, solidified by liquid-phase sintering, crushed, and gap-graded for use in high-strength DUCRETE at 5000 to 6000 psi, (35–42 MPa)

DUCRETE Casks are Considerably Smaller and Lighter than Casks Constructed of Ordinary Concrete

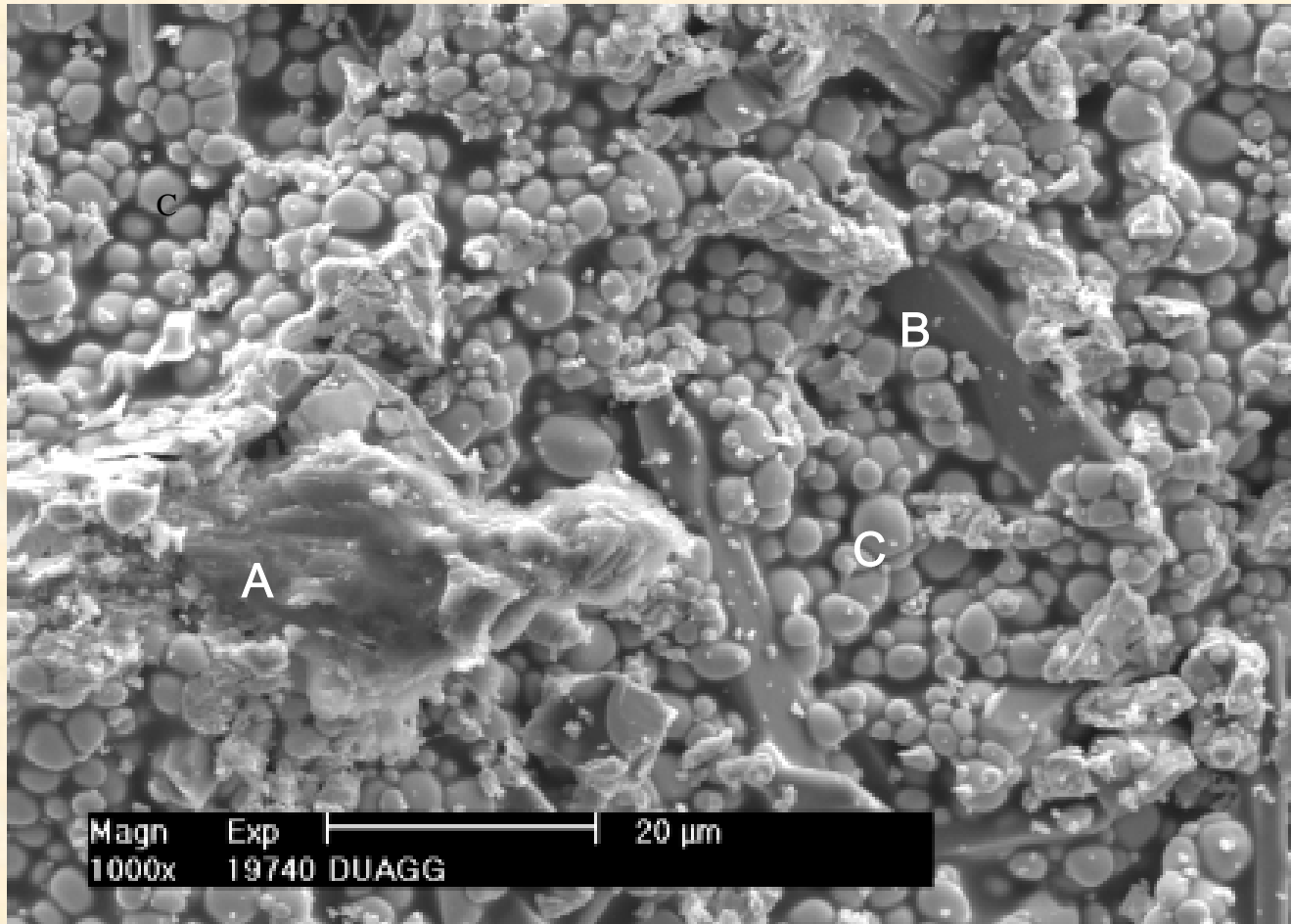
The DUCRETE cask is 35 tons lighter and 100 cm smaller in diameter than casks made from ordinary concrete.



Comparison of conventional and DUCRETE spent-fuel dry storage casks/silos



View of DUAGG Before Testing



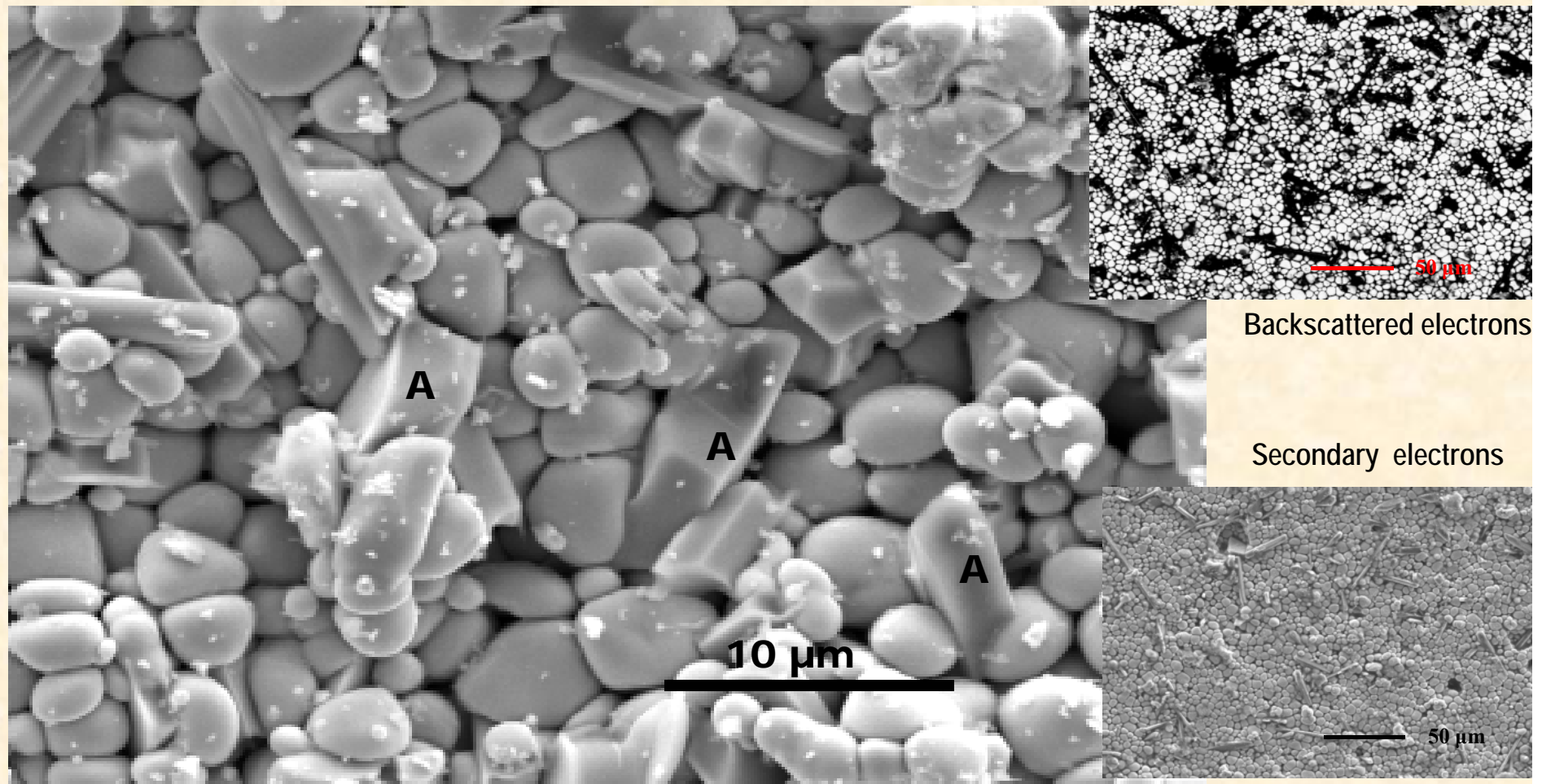
Detail of the surface (secondary electrons)

Particle A contains Al

Particle B contains Ti and some Mg

Area C contains DUO_2 particles surrounded by dark basalt

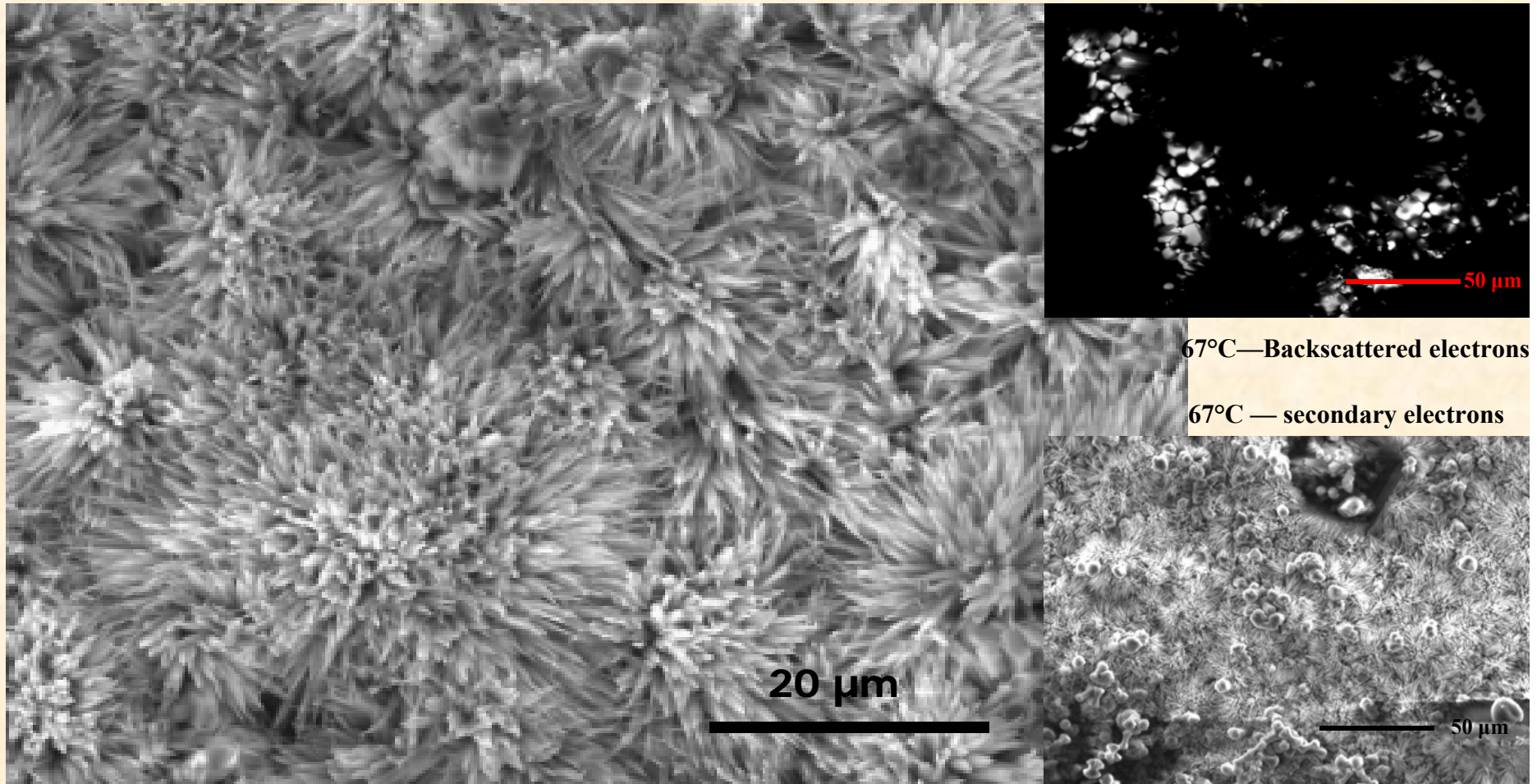
DUAGG after 6 Months in DI Water



150°C — secondary electrons

Particles A contain Ti and some Mg

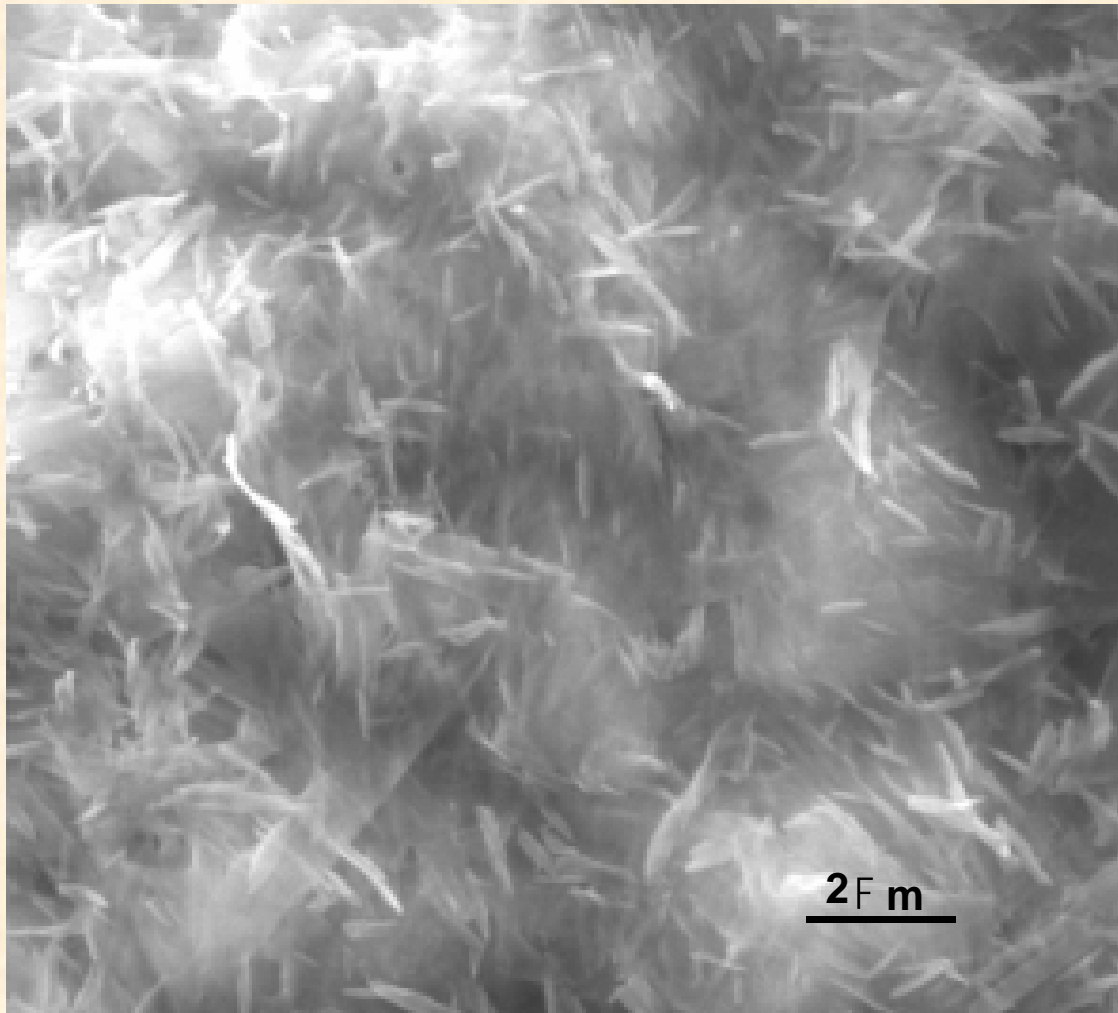
DUAGG after 6 Months in Cement Pore Solution



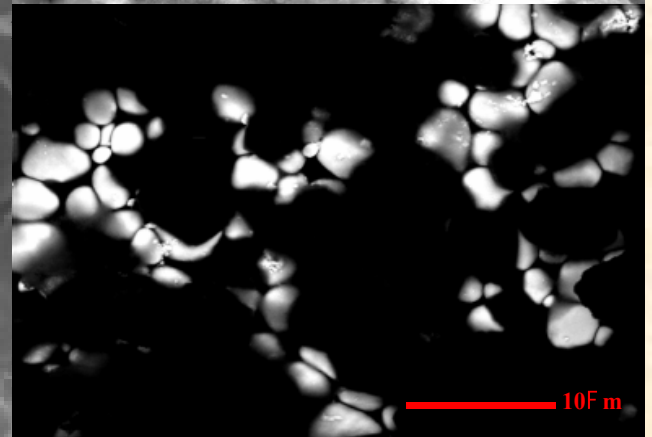
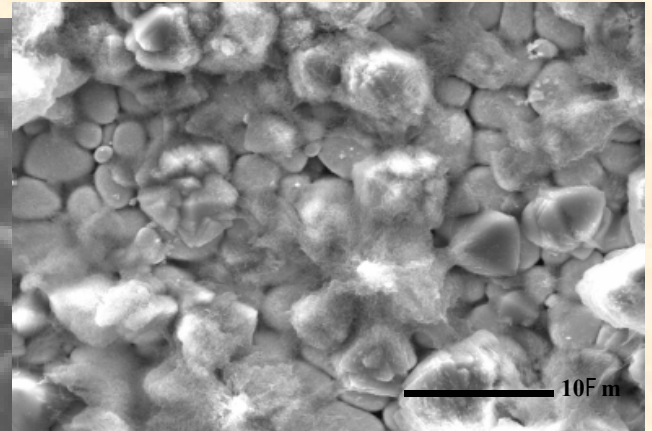
67°C — secondary electrons

Covered by CaCO₃ and needle-like crystals containing Ca, Si, and some Al

DUAGG after 6 Months in Cement Pore Solution



150 C secondary electrons

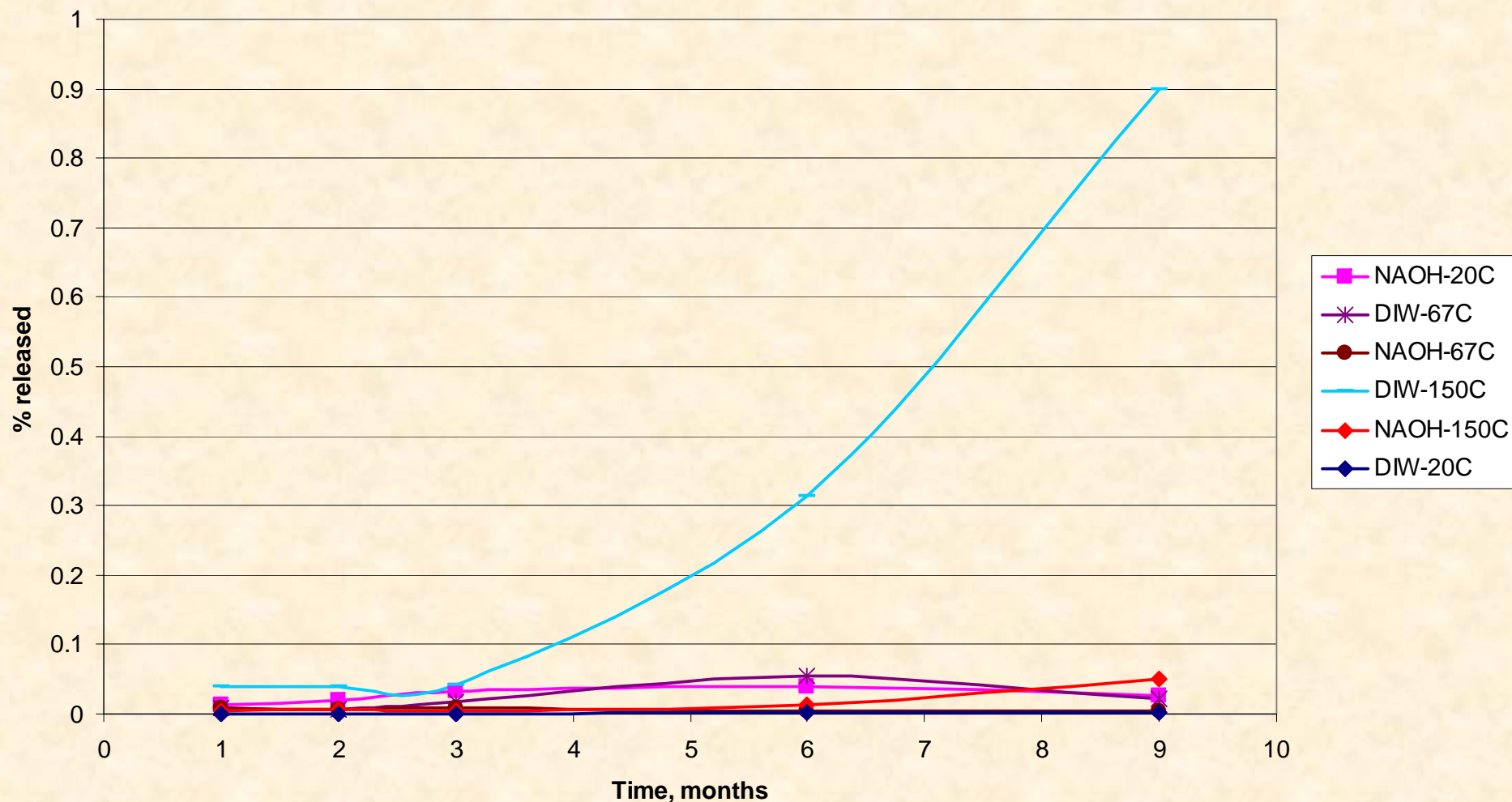


150 C backscattered electrons

Cement hydration products cover surface with phases with Ca, Si, and Al.

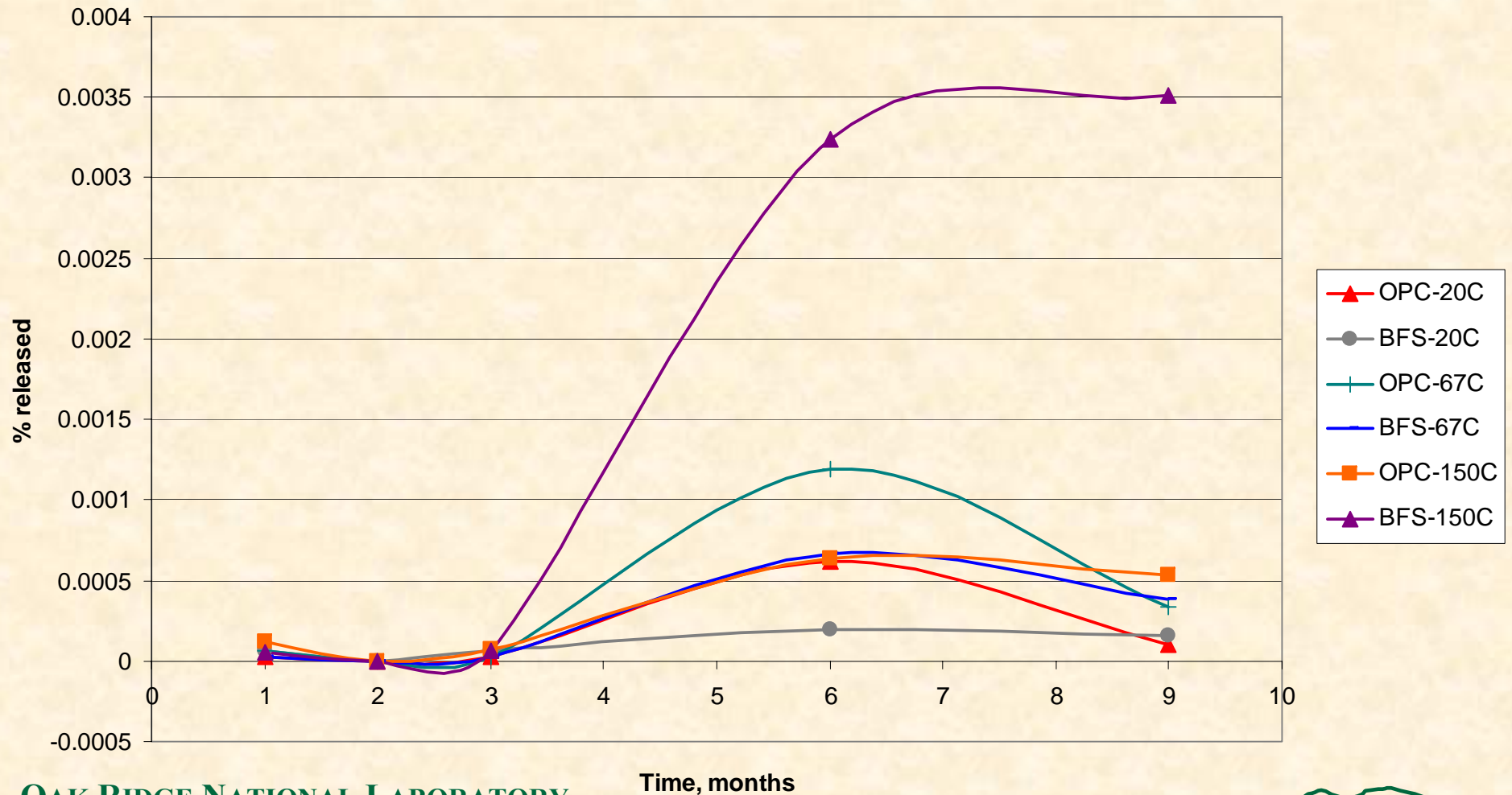
U Released from High-Fired UO_2 Fuel Pellet into 1 N NaOH and Distilled Water

Uranium released (%) from DUO_2 pellet

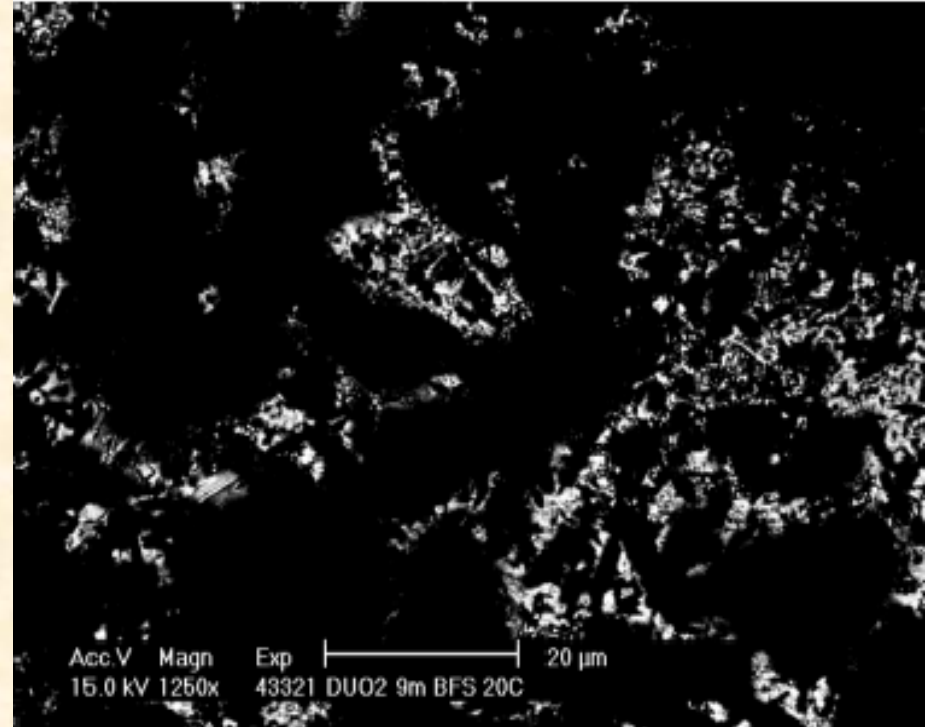
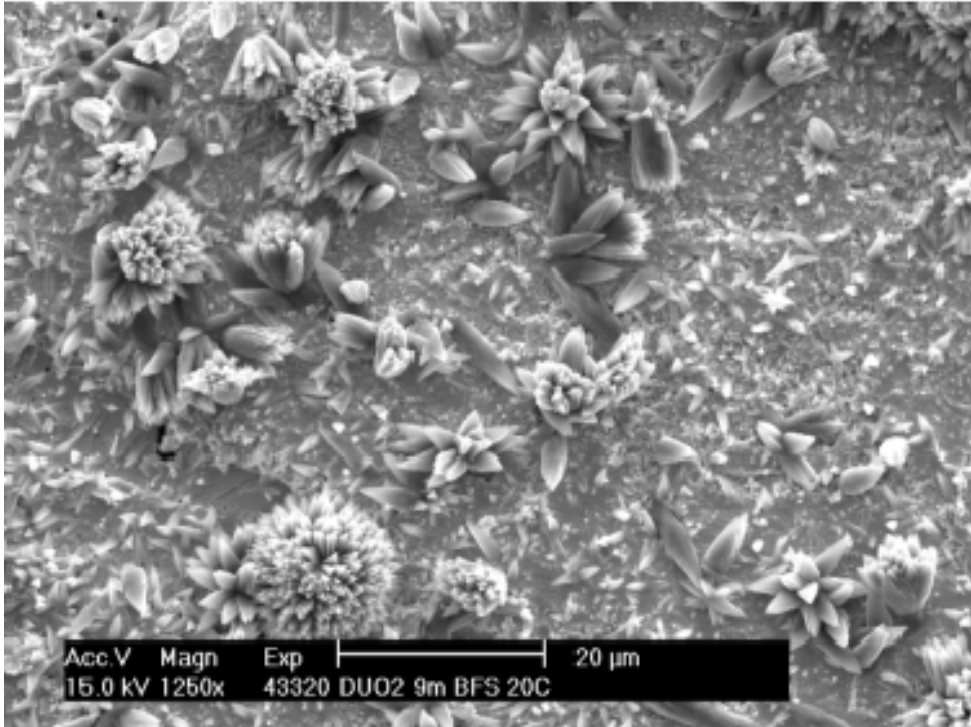


U Released from High-Fired UO_2 Fuel Pellet into Cement and Slag Porewater

Uranium released (%) from DUO2 pellet

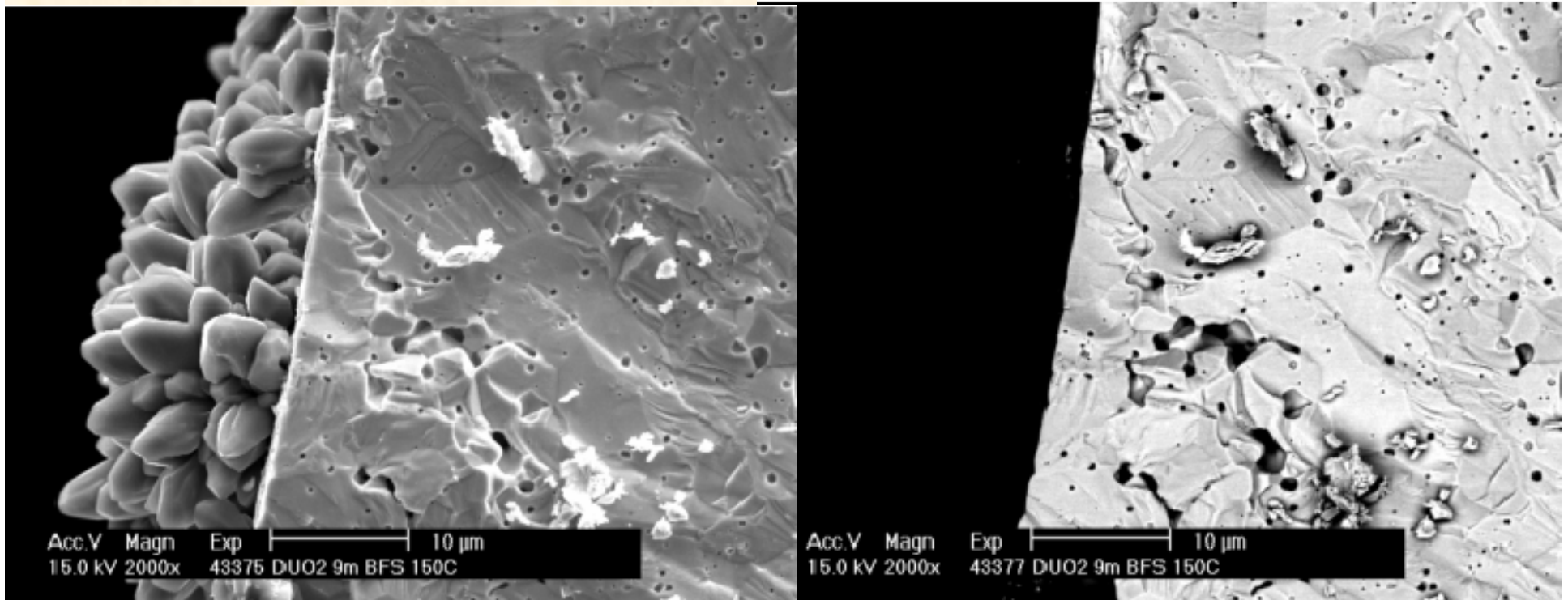


High-Fired DUO₂ Fuel Pellet in 60% OPC + 40% BFS Porewater at 20°C for 9 Months



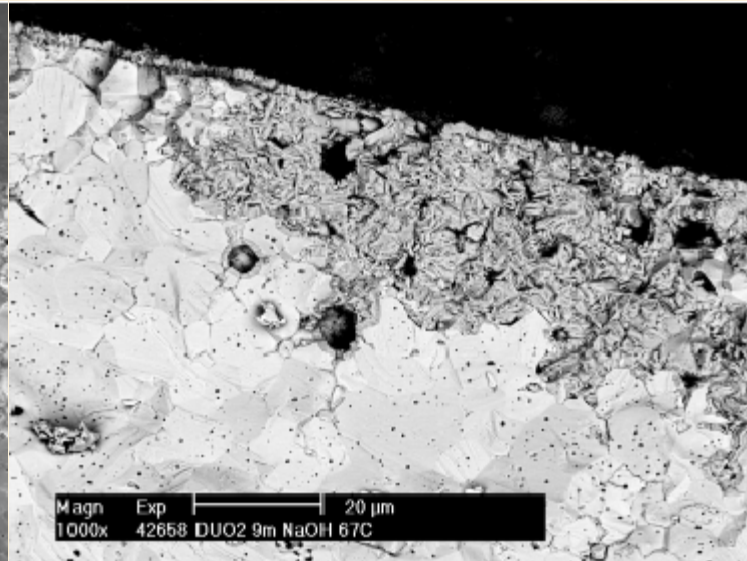
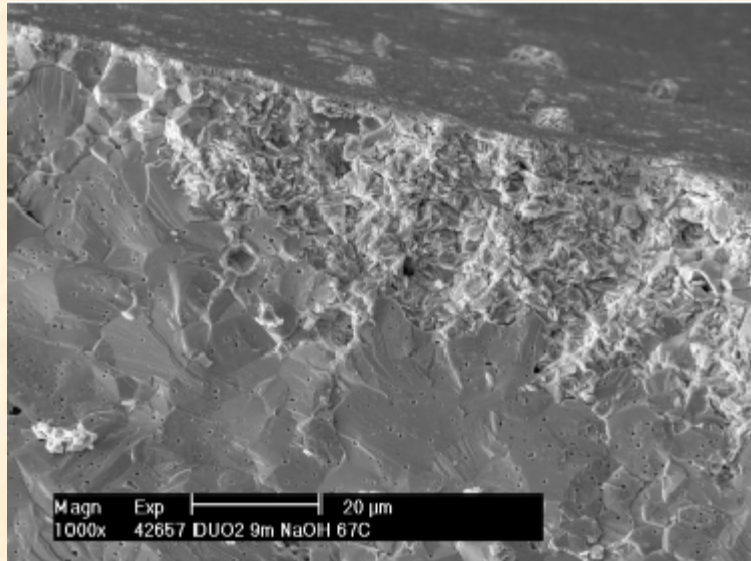
Side view with CaCO₃ deposits

High-Fired DUO₂ Fuel Pellet in 60% OPC + 40% BFS Porewater at 67°C for 9 Months

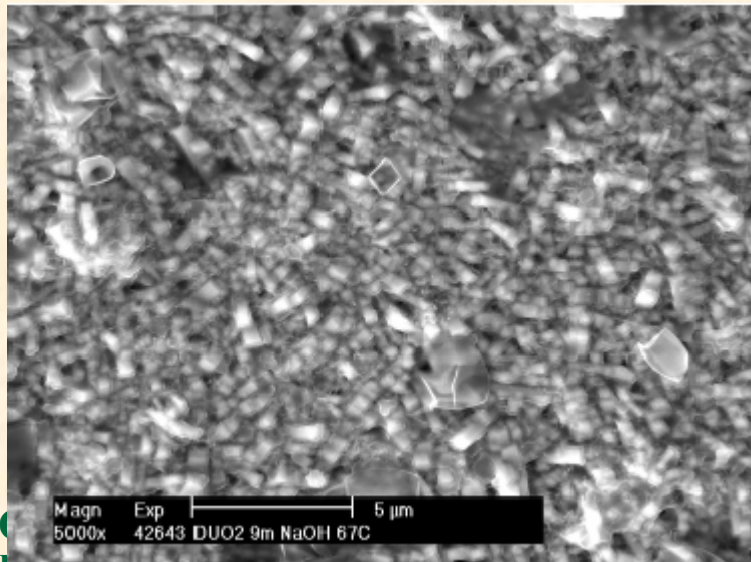


Fracture of the cylinder - CaCO₃ visible on the outside surface

High-Fired DUO_2 Fuel Pellets in 1N NaOH Solution at 67°C for 9 Months

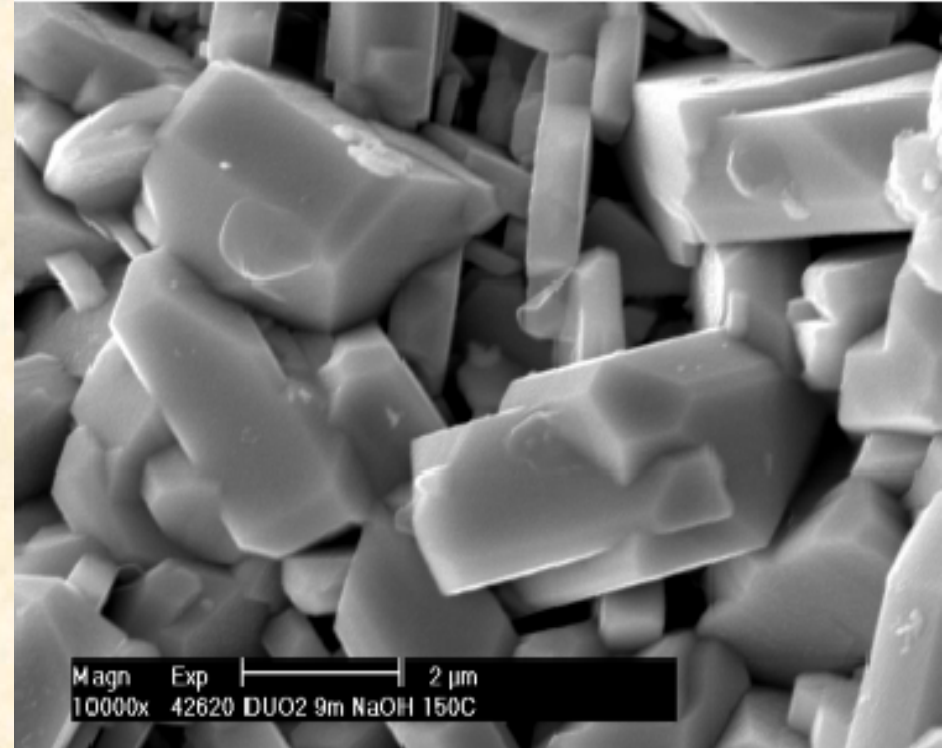
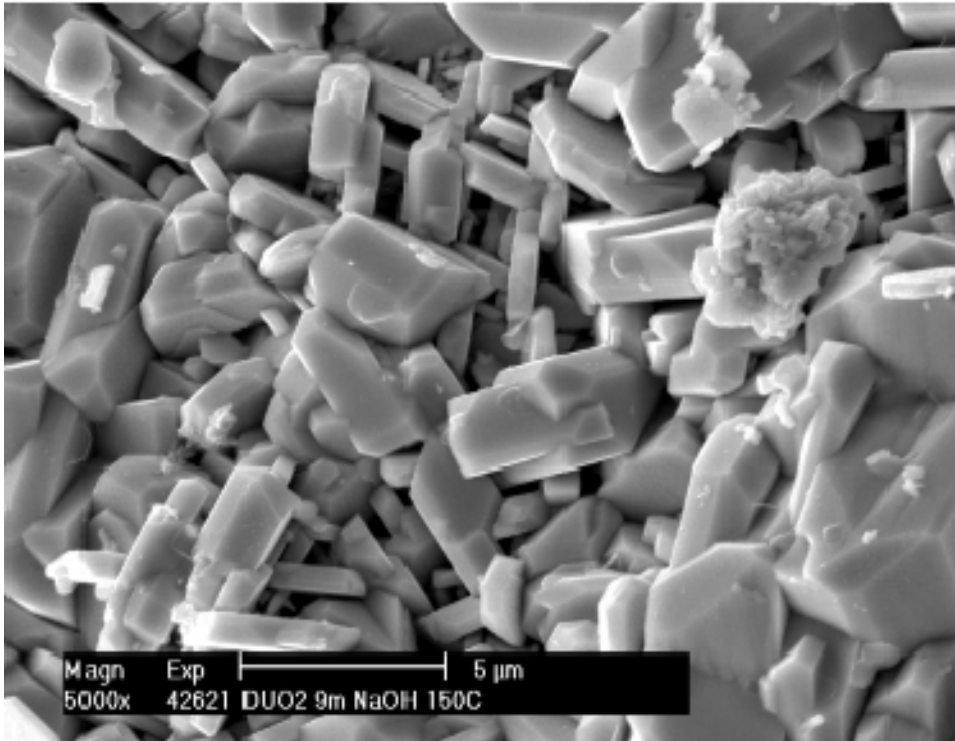


Fracture



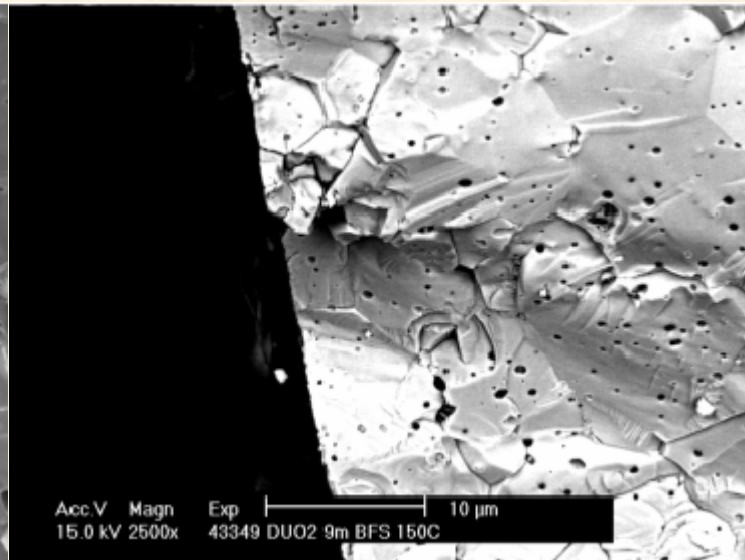
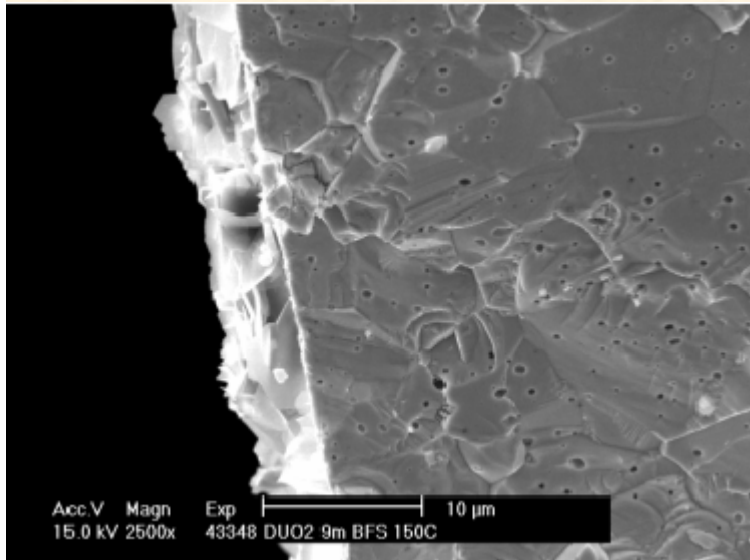
Side

High-Fired DUO_2 Fuel Pellets in 1N NaOH Solution at 150°C for 9 Months

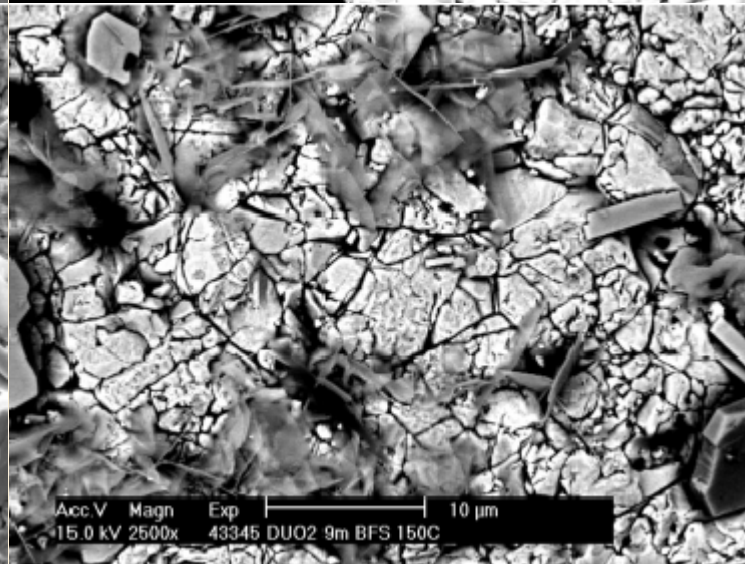
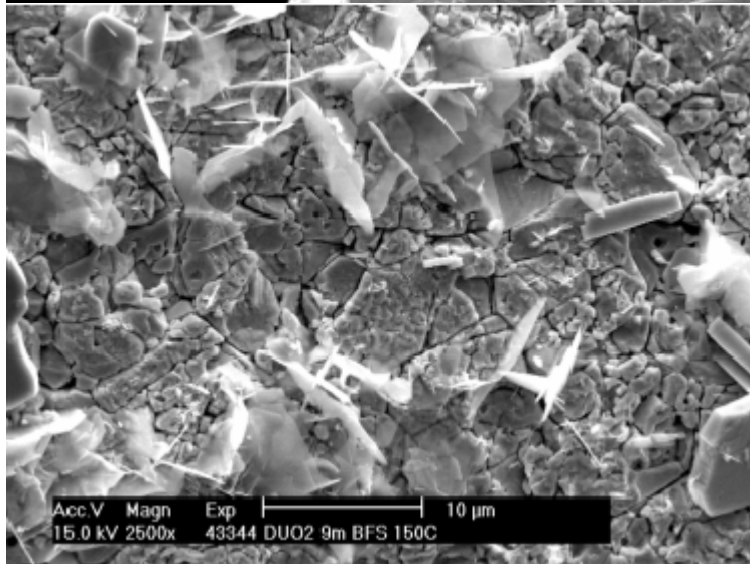


Side of the exposed fuel-pellet shows grains of DUO_2 that are not cohesive

High-Fired DUO₂ Fuel Pellet in 60% OPC + 40% BFS Porewater at 150°C for 9 Months



Fracture

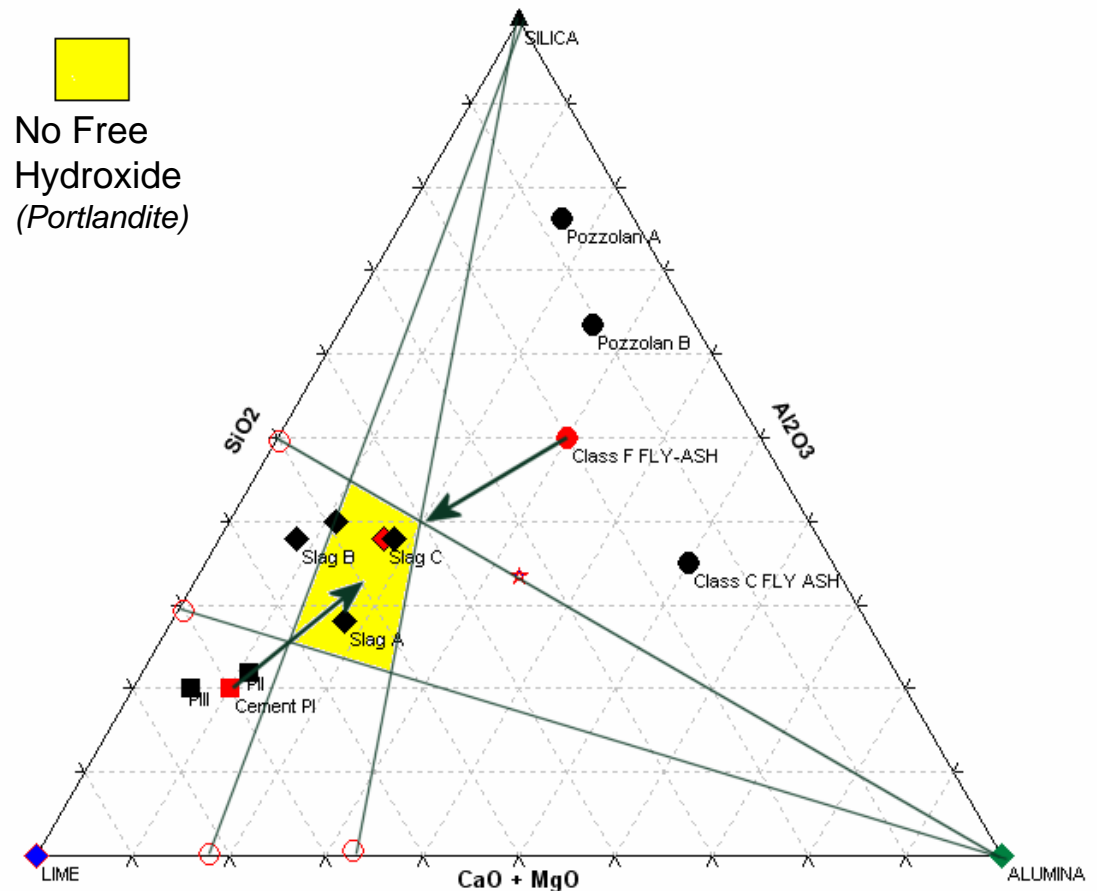


Top

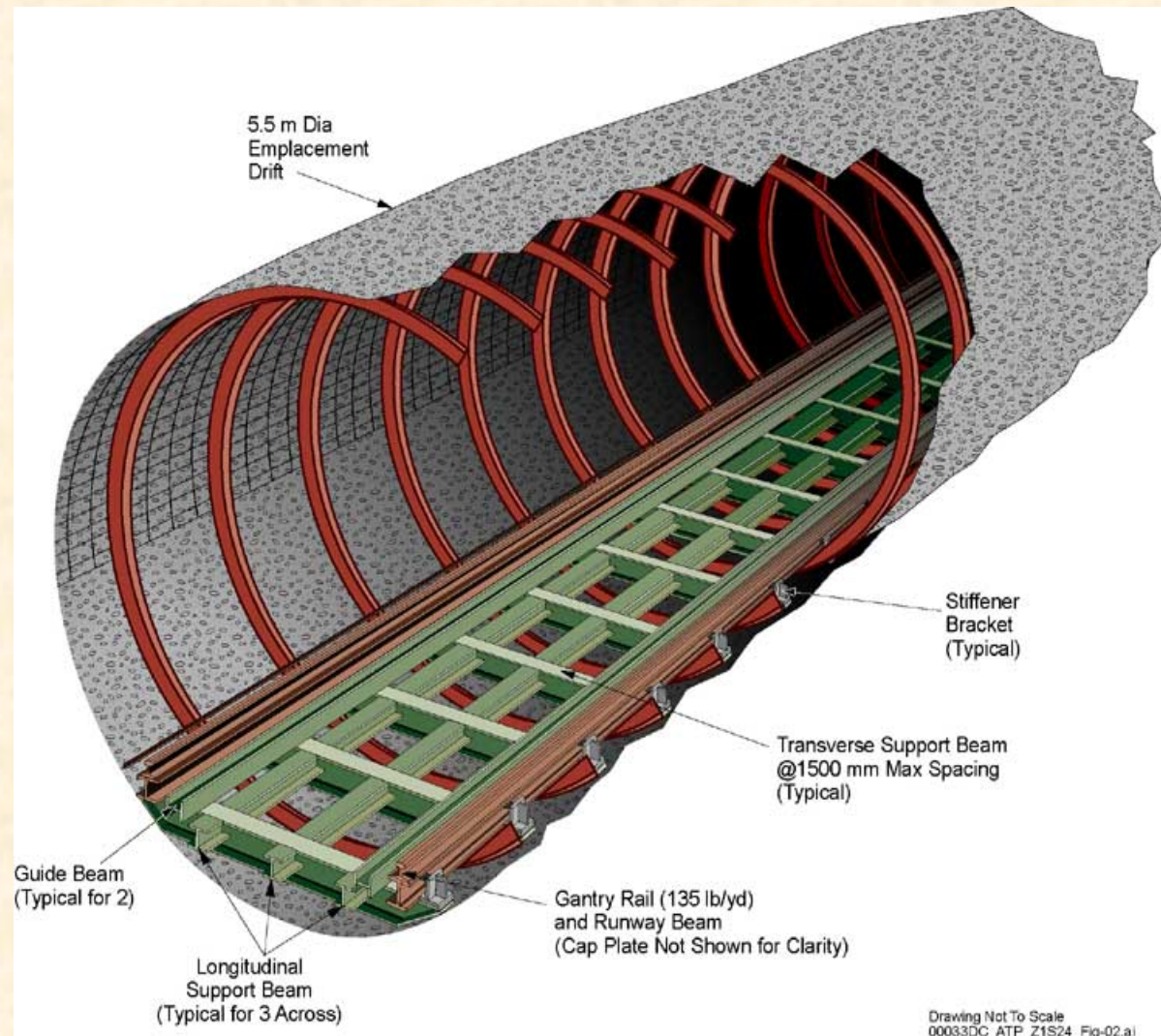
Cementitious Material Compatible with Yucca Mountain Geochemistry

LR Dole, CH Mattus, LR Riciputi, M Fayek, L.M. Anovitz, D Olander, S Ermichev, and VI Shapovalov

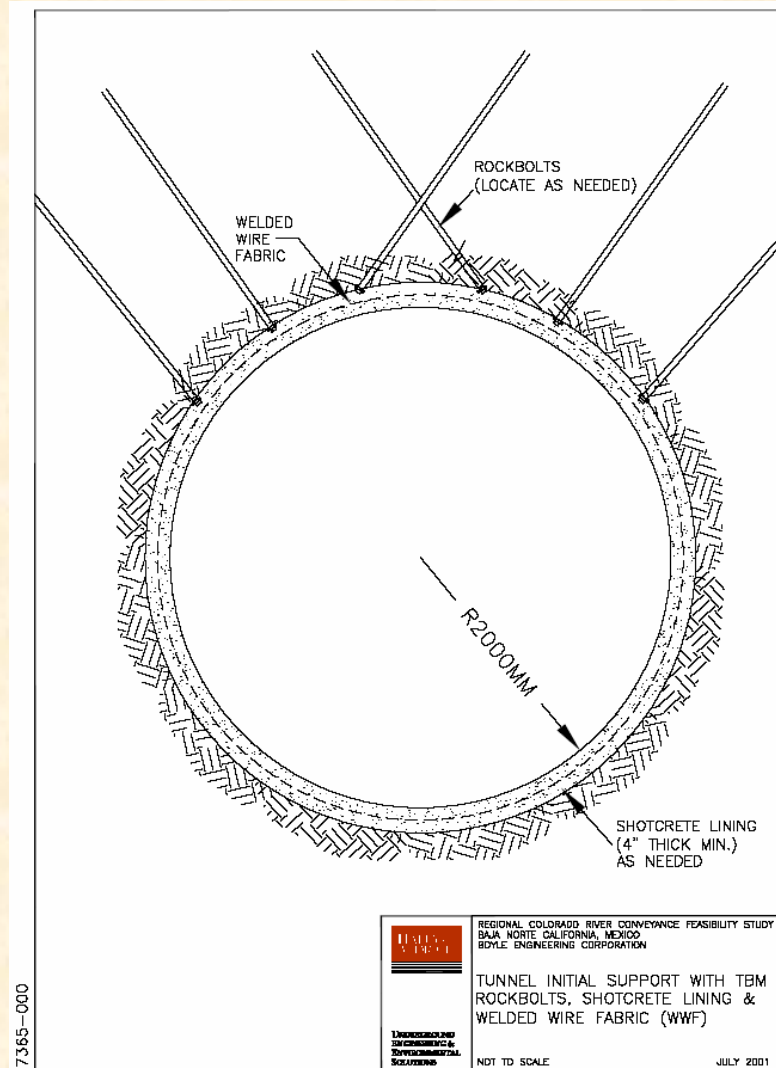
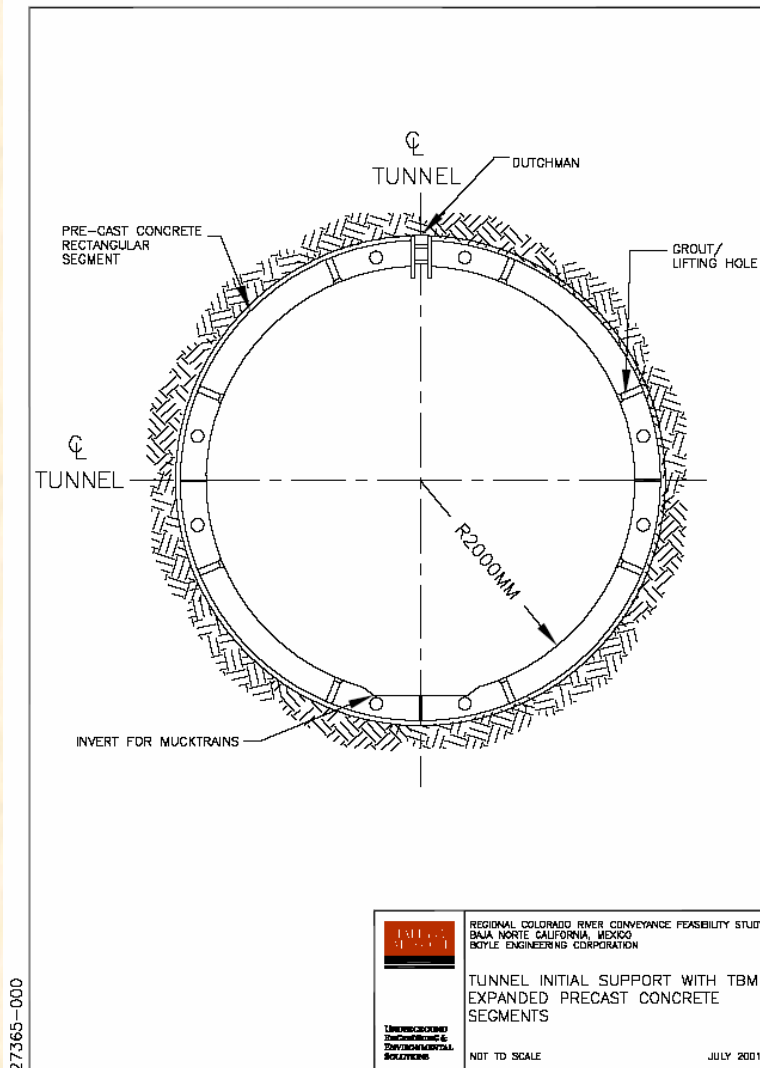
- **Select durable low-pH cement/concrete formulas based on materials science, thermodynamic modeling, and experience**
- **Test mechanical properties and chemical interactions with YMP brines under expected service conditions**
- **Compare results with**
 - Ancient cements (2–6 Ky)
 - Natural cements (>100 My)
- **Calculate impacts on improving YMP construction costs and reducing risks**



Replace Current Steel YM Tunnel Liners



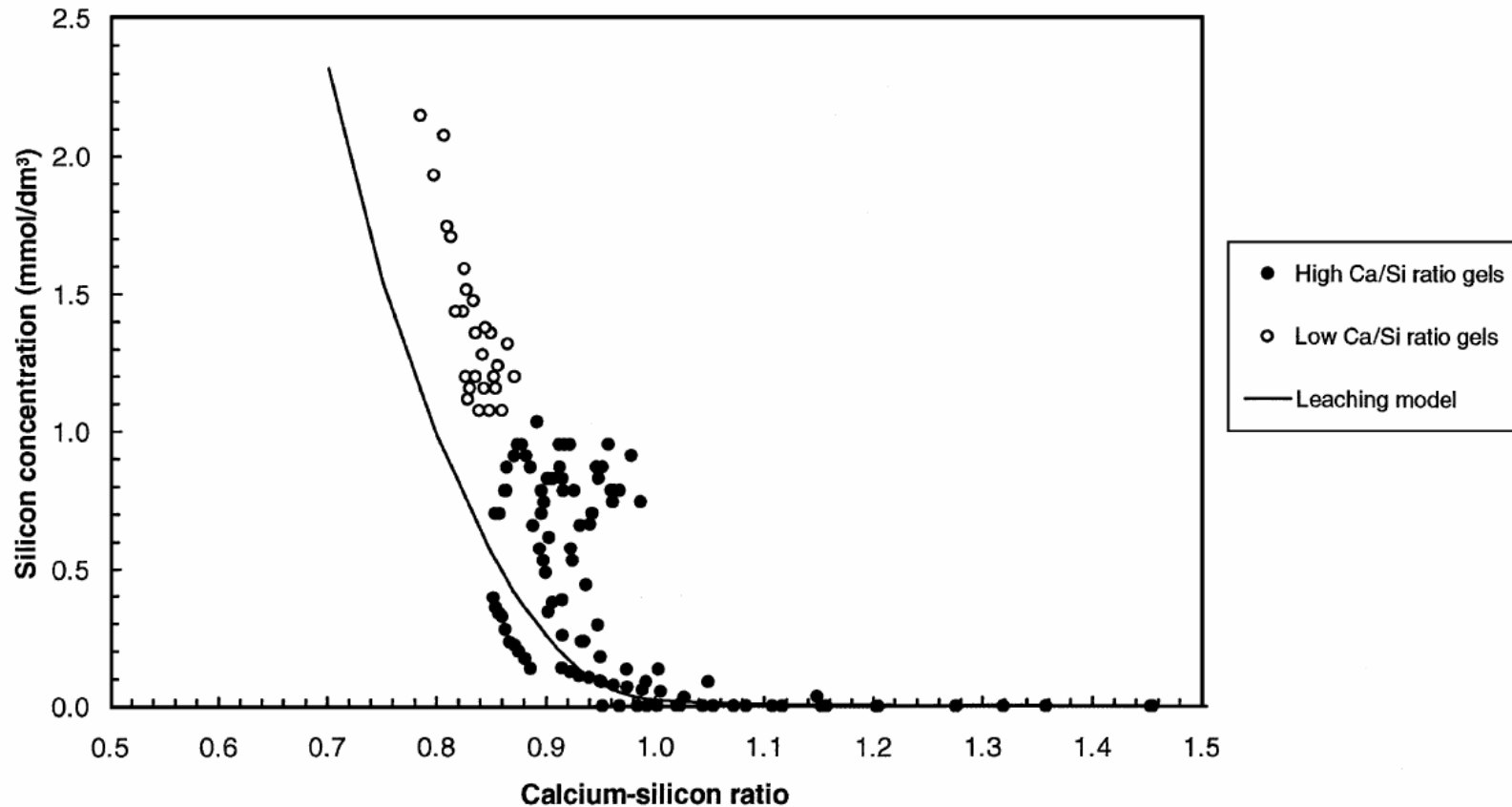
Replace with Cement Liners: Pre-Cast, Cast-In-Place, and/or Shotcrete



Five YMP Historical Issues with Cementitious Construction Materials

YMP Model Assumptions	Mitigated by High-Silica Cements
Concrete pore solutions with a high pH could increase radionuclide solubility and mobility	High-silica cements reduce the pH of leachates that then react to form insoluble silicates
Water from dehydration of concretes increase the relative humidity in tunnels and drifts	Very fine capillary texture of high-silica cements will minimize moisture loss
The porosity, permeability, and transport properties of the adjacent formation could be changed to effect higher nuclide transport rates	Silica saturated leachates will reduce the porosity and permeability in the adjacent the vitreous tuff
Superplasticizers in the concrete matrix could form organic acids increasing nuclide transport	High-silica additives are water-reducers and lessen or eliminate the need for organic-surfactant additives
Organics and sulfate in the concretes could provide nutrients for microbiological growth accelerating corrosion of the waste packages	Can support colonies of biota, but microorganisms cannot extract nutrients from high-silica cements

Increasing Silica in Cement Increases Silica in Leachates



Harris, A.W., M.C. Manning, W.M. Tearle, and C.J. Tweed, Testing of models of the Dissolution of cements—leaching of synthetic CSH gels, Cement and Concrete Research, 32, pp 731–746, 2002.

Saito, Hiroshi and Akira Deguchi, Leaching tests on different mortars using accelerated electrochemical method, Cement and Concrete Research 30, pp 1815-1825, 2000.

Figure (a)
These plots show the pore size distributions in normal sand filled cement mortars

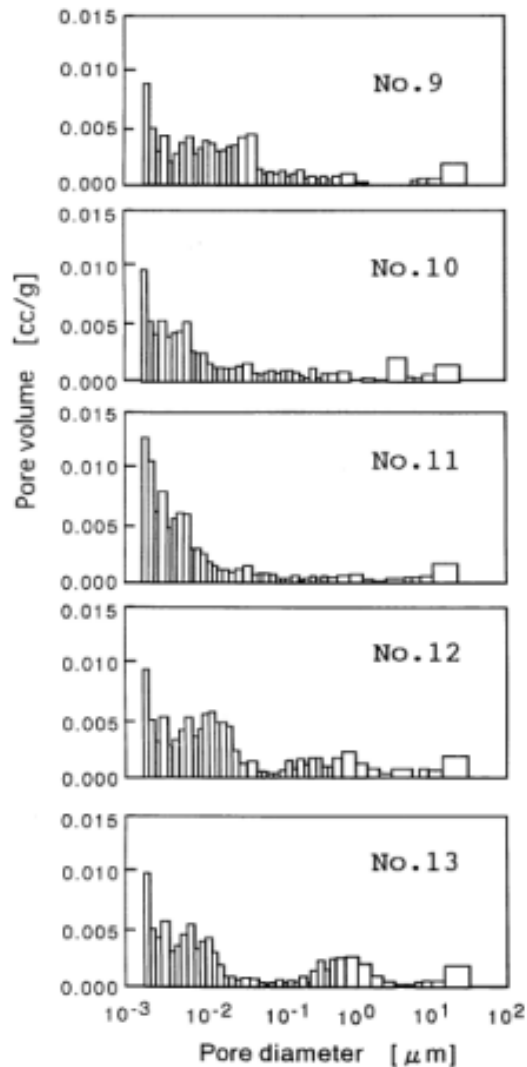
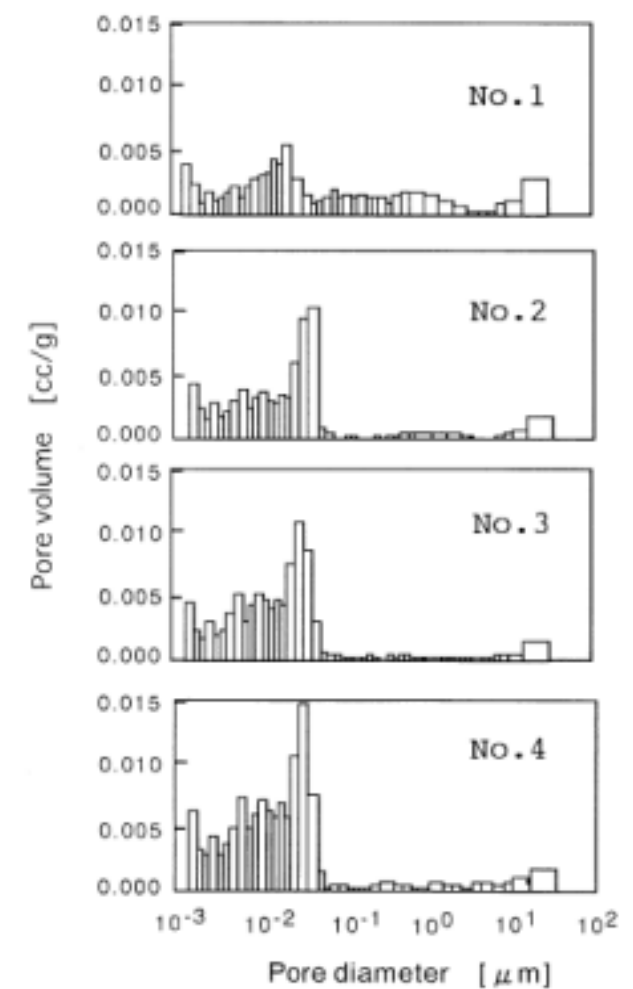


Figure (b)
Additions of blast furnace slag and silica fume significantly reduce the pore sizes



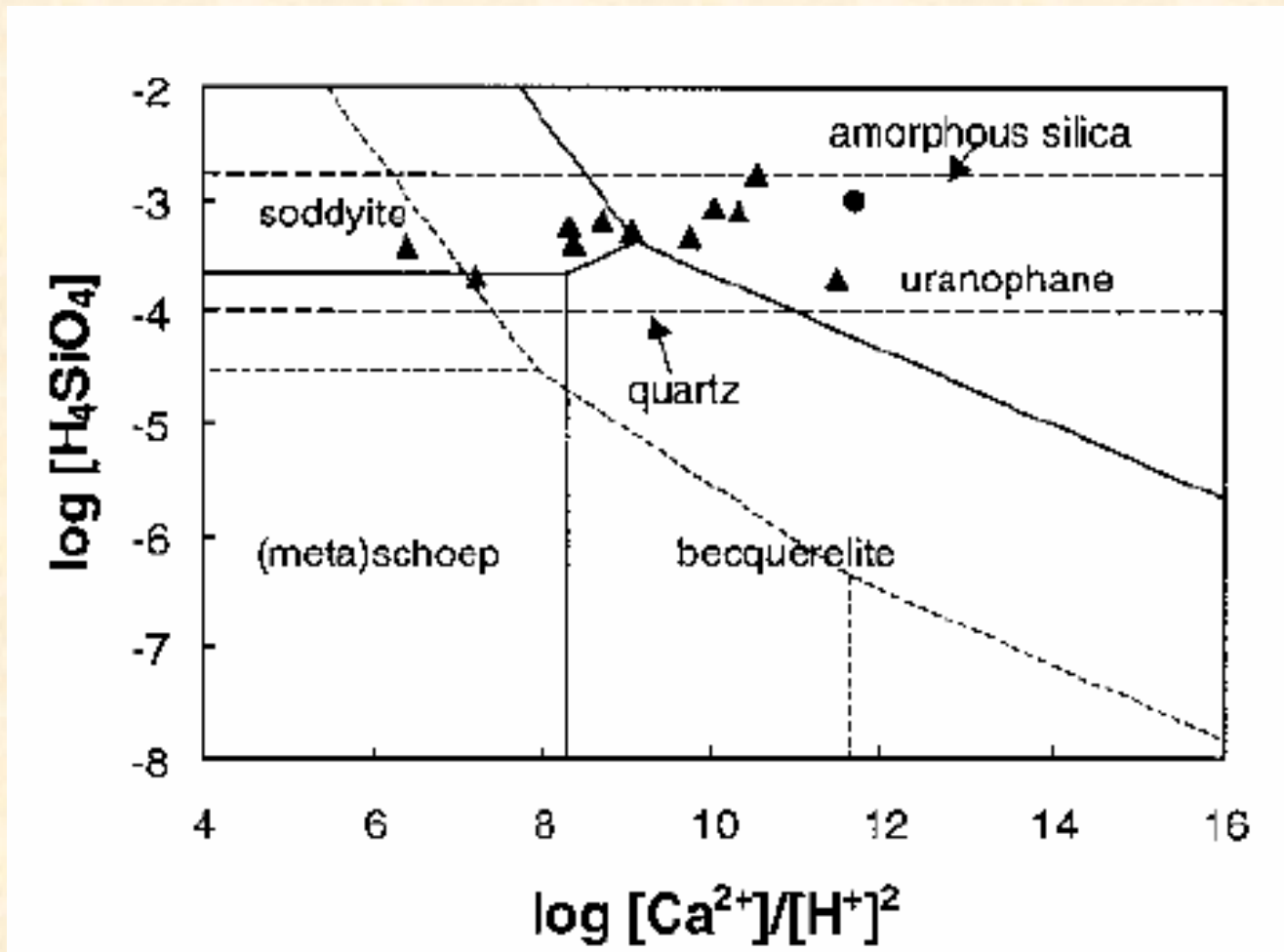
Principal U(VI) Compounds

Values of $\Delta G_{f,298}^{\circ}$ for the U(VI) minerals used in the construction of Fig. 7 (Chen 1999)

Uranyl phases	Formula	kJoule/mol ^a	kJoule/mol ^b
Metaschoepite	$[(\text{UO}_2)_8\text{O}_2(\text{OH})_{12}] \cdot (\text{H}_2\text{O})_{10}$	-13,092.0	-13,092.0
Becquerelite	$\text{Ca}[(\text{UO}_2)_6\text{O}_4(\text{OH})_6] \cdot (\text{H}_2\text{O})_8$	-10,324.7	-10,305.8
Rutherfordine	UO_2CO_3	-1,563.0	-1,563.0
Uranocalcarite	$\text{Ca}_2[(\text{UO}_2)_3(\text{CO}_3)(\text{OH})_6] \cdot (\text{H}_2\text{O})_3$	-6,036.7	-6,037.0
Sharpite	$\text{Ca}[(\text{UO}_2)_6(\text{CO}_3)_5(\text{OH})_4] \cdot (\text{H}_2\text{O})_6$	-11,607.6	-11,601.1
Fontanite	$\text{Ca}[(\text{UO}_2)_3(\text{CO}_3)_4] \cdot (\text{H}_2\text{O})_3$	-6,524.7	-6,523.1
Liebigite	$\text{Ca}_2[(\text{UO}_2)(\text{CO}_3)_3] \cdot (\text{H}_2\text{O})_{11}$	-6,446.4	-6,468.6
Haiweeite	$\text{Ca}[(\text{UO}_2)_2(\text{Si}_2\text{O}_5)_3] \cdot (\text{H}_2\text{O})_5$	-9,367.2	-9,431.4
Ursilite	$\text{Ca}_4[(\text{UO}_2)_4(\text{Si}_2\text{O}_5)_5(\text{OH})_6] \cdot (\text{H}_2\text{O})_{15}$	-20,377.4	-20,504.6
Soddyite	$[(\text{UO}_2)_2\text{SiO}_4] \cdot (\text{H}_2\text{O})_2$	-3,653.0	-3,658.0
Uranophane	$\text{Ca}[(\text{UO}_2)(\text{SiO}_3\text{OH})_2] \cdot (\text{H}_2\text{O})_5$	-6,192.3	-6,210.6

^a Chen 1999 ^b Finch 1997

High-Silica Forces Formation of Insoluble Uranium Silicates



Silicates Form a Dense Diffusion Layer on the Surface of UO_2 Even Under Oxidizing Conditions

